Inelastic-neutron-scattering investigation of the spin-Peierls system $CuGeO_3$

L. P. Regnault
Département de Recherche Fondamentale sur la Matière Condensée, Service de Physique Statistique, Magnétisme et Supraconductivité, Laboratoire de Magnétisme et Diffraction Neutronique, Centre d'Etudes Nucléaires, 38054 Grenoble cedex 9, France

M. Aïn and B. Hennion
Laboratoire Leon Brillouin, Centre d'Etudes de Saclay, 91191 Gif sur Yvette Cedex, France

G. Dhalenne and A. Revcolevschi
Laboratoire de Chimie des Solides, Université de Paris Sud, Bâtiment 414, 91405 Orsay, France
(Received 10 July 1995)

We have investigated the spin dynamics of the spin-Peierls system $CuGeO_3$ by inelastic neutron scattering. The measurements have been performed as a function of wave vector, temperature, and magnetic field, for fields perpendicular to the chain axis (up to 10 T). Our neutron results confirm the occurrence of a crystalline distortion below $T_{SP}\approx 14.2$ K, corroborated by the appearance of superlattice peaks indexed with a commensurate wave vector $\mathbf{k}_{SP}=(\frac{1}{2},0,\frac{1}{2})$. At low temperature, the spin-excitation spectrum exhibits a well defined energy gap $\Delta\approx 2$ meV$\approx 1.66\, kT_{SP}$ at the antiferromagnetic point $\mathbf{k}_{AF}=(0,1,\frac{1}{2})$, distinct from $\mathbf{k}_{SP}$. The experimental results for $T\ll T_{SP}$ are quantitatively understood from an alternating-exchange Hamiltonian with an exchange parameter $(2J_1)\approx 10.6$ meV and an alternation parameter $\alpha=J_2/J_1\approx 0.92$, despite the existence of sizable interchain couplings both along the a and b axes ($J'_a/J_1\approx 0.011$ and $J'_b/J_1\approx 0.11$, respectively). We present the temperature dependence of the spin dynamics on both sides of T_{SP}. Our results confirm the persistence of a pseudogap in the excitation spectrum for $\mathbf{q}=\mathbf{k}_{AF}$, but only in the immediate vicinity of the spin-Peierls transition temperature. The pseudogap vanishes rapidly with T, following decreasing size of dimerized segments. The stronger inelasticity observed above T_{SP} at $\mathbf{q}=\mathbf{k}_{SP}$ has been attributed to an effect of the dispersion of magnetic excitations due to interchain couplings J'_a and J'_b. Under a magnetic field applied perpendicular to the chain axis, the excited triplet is split into three components, with gap values depending linearly on the field. The spin-Peierls transition temperature T_{SP} decreases with increasing field, following a quadratic dependence on H, in agreement with theoretical as well as other experimental results. We have determined the field dependence of the dimerization peak intensities up to 10 T, which show very small changes. In particular, no trace of pretransitional incommensurability could be detected, at least up to $0.77H_c$.

I. INTRODUCTION

By now, it is well established[1–4] that at $T=0$ the ideal spin-1/2 one-dimensional Heisenberg antiferromagnetic (1D-HAF) system described by the simple isotropic Hamiltonian $H=2J\Sigma_i \mathbf{S}_i\cdot\mathbf{S}_{i+1}$, where J is the nearest-neighbor intrachain coupling constant, is characterized by a gapless continuum of magnetic excitations and by a slowly decaying spin-spin correlation function given by the relation (neglecting logarithmic corrections) $\langle \mathbf{S}_0\cdot\mathbf{S}_r\rangle \propto (-)^r/r$. The correlation length is infinite at $T=0$, but the ground state is not magnetically ordered at long range as a result of quantum fluctuations. It is also well admitted[5–8] that such a uniform chain is unstable when coupled to a three-dimensional (3D) phonon field. This coupled system undergoes, at some finite temperature T_{SP} [called the spin-Peierls (SP) transition temperature] a crystalline distortion which transforms the uniform chain into a chain of coupled dimers. The resulting lattice dimerization is characterized by the appearance in the reciprocal space of superlattice peaks around the ''normal'' nuclear Bragg peaks, described by a 3D propagation vector hereafter defined as $\mathbf{k}_{SP}$. This distortion induces changes both in the lattice and spin dynamics. Concerning the former, the main consequence is the prediction at $\mathbf{q}=\mathbf{k}_{SP}$ of a softening in the phonon branch involved in the lattice distortion as $T\rightarrow T_{SP}$. Concerning the magnetic counterpart, the most important consequence of the lattice distortion is the progressive establishing of alternating exchange along the chain as $T\rightarrow 0$. At low temperatures (i.e., when $T\ll T_{SP}$) and neglecting all interchain magnetic couplings, the Hamiltonian describing the dimerized spin system can be mapped onto the Hamiltonian of a spin-1/2 alternating antiferromagnetic chain:[9]

$$H=2J_1\sum_i (\mathbf{S}_{2i}\cdot\mathbf{S}_{2i+1}+\alpha\mathbf{S}_{2i+1}\cdot\mathbf{S}_{2i+2}), \qquad (1)$$

which now depends, in the simplest case, on two different alternating exchange constants J_1 and $J_2=\alpha J_1$ instead of one in the original (high-temperature) uniform chain. The parameter α, called the alternation parameter, characterizes the relative strengths of exchange couplings ($\alpha<1$ by definition). The coupling constants J_1 and J_2 can be expressed in a different way by introducing the lattice distortion δ, usually defined in the literature as[5,9]

$$J_1 = J(1+\delta),$$

$$J_2 = J(1-\delta), \tag{2}$$

where J is the average exchange value [$J=(J_1+J_2)/2$]. In the most general case, δ should be a function of displacement vectors $\boldsymbol{\delta}_i$ associated with the various atomic entities involved in the intrachain exchange paths. Moreover, in the SP problem J, α, and δ must depend on temperature to account for the inherent lattice effects. The simple expression $\delta=(1-\alpha)/(1+\alpha)$ relates the alternation α and distortion δ.

As for the magnetic excitation spectrum of an alternating chain, it is expected for a SP system that a gap Δ (function of J_1 and α or, equivalently, J and δ) opens at the antiferromagnetic point $\mathbf{k}_{\mathrm{AF}}$ between a *nonmagnetic* singlet ($S=0$) ground state and the ''continuum'' of lowest-excited triplet ($S=1$) states.[9–11] $\mathbf{k}_{\mathrm{AF}}$ is frequently defined as the point ''$q=\pi$'' in the literature. The reduced gap $\Delta/2J_1$ has been calculated numerically[9–13] for an alternating chain as a function of the alternation parameter α. For not too large values of $1-\alpha$, this ratio is given by the simple power-law function $\Delta/2J_1 \approx c(1-\alpha)^{\nu}$ with a prefactor $c\approx 1$ and an exponent $\nu\approx 2/3$ in case of isotropic spins.[7,13] For the SP problem in the mean-field approximation, a linear relation $\Delta\approx 1.64(2J)\delta$ has been predicted by Pytte[5] between Δ and δ. However, in the more sophisticated approach of Cross and Fischer,[7] the completely different relation $\Delta\propto(2J)\delta^{2/3}$ has been deduced, which agrees better with the expected equivalent alternating-chain problem. In the mean-field approximations, Δ and T_{SP} appear directly related by a BCS-type relation[5]

$$2\Delta \approx 3.53 k T_{\mathrm{SP}}, \tag{3}$$

which results essentially from the treatment of the spin-phonon interaction in the weak-coupling limit.

An important consequence of both the singlet ground state and the presence of a gap is that no long-range magnetic ordering should exist, in the ideal system, even at $T=0$. This ought to be true also for a nonideal system, as a result of the finite intrachain magnetic correlation length ξ (typically one expects $\xi^{-1}\approx\Delta/c_0$, where c_0 is the spin-wave velocity, defined for a spin-1/2 HAF system by $c_0\approx\pi Jd$, d being the intrachain spacing), which leaves the SP-coupling mechanism largely unaffected by any *sufficiently small* interchain coupling J'. A practical consequence of the existence of both a singlet ground state and a gap is the prediction of an exponential dependency at low temperatures of quantities like, e.g., $\chi(T)$, $C(T)$, $1/T_1T$,... which can be checked experimentally.

The properties of a SP system in a magnetic field H have been discussed by several authors.[14–16] According to these theories, the transition temperature T_{SP} is predicted to decrease as the field increases, following a quadratic relation at low fields[14,15] ($\Delta T_{\mathrm{SP}}/T_{\mathrm{SP}}\propto -H^2$). At larger fields and low temperatures, when H reaches some critical value H_c, the nonmagnetic SP system is expected to enter a new *magnetic* intermediate phase, the nature of which is not completely elucidated.[8,15–17] In particular, this phase should be characterized by the coexistence of both a uniform (at $q=0$) and a staggered magnetization up to a second characteristic field H_{c2}, above which the saturated paramagnetic state is reached. Moreover, this phase should remain distorted, the lattice distortion being more likely incommensurate in this part of the H-T phase diagram.[8,15–17] The magnetic staggered short-range correlations are also expected to become incommensurate above the critical field, as for the alternating chain system. H_c has been calculated in mean-field approximation, giving at $T=0$[15,16]

$$g\mu_B H_c/2kT_{\mathrm{SP}} \approx 0.74 \tag{4a}$$

or equivalently, using relation (3)

$$g\mu_B H_c/\Delta \approx 0.84. \tag{4b}$$

Unfortunately, little is known in the literature concerning the field dependencies of the magnetic gap $\Delta(H)$ or the lattice distortion $\delta(H)$ and their relationship. In zero field and for small lattice distortions, one has a direct relation between Δ and δ: $\Delta(0)\propto[\delta(0)]^{\nu}$. As previously discussed, the value of the exponent ν depends strongly on the spin dimensionality, with $\nu=2/3$ for Heisenberg spins[15] and $\nu=1$ for the exactly solvable $S=1/2$ XY model.[9] Such a simple relation is no longer true under the field. Indeed, from very general arguments[18,19] the lowest excited $S=1$ triplet should split into three distinct components (labeled hereafter as Δ_-, Δ_0, and Δ_+). The lowest energy gap $\Delta_-(H)$ is expected to vary linearly with H in a first approximation (following the relation $\Delta_-(H)\approx\Delta-g\mu_B H$), and should vanish at a critical field $H_c\approx\Delta/g\mu_B$, above which the incommensurate magnetic phase takes place. This is the situation expected to occur for an alternating chain with negligible spin-lattice interactions.[20] In the SP problem, nonlinear effects originating from the spin-lattice couplings should occur in the vicinity of H_c to account for the fact that $g\mu_B H_c$ is slightly (16%) smaller than Δ [see Eq. 4(b)], although the gap is still expected to vanish at H_c [$\Delta_-(H_c)=0$]. On the other hand, $T_{\mathrm{SP}}(H_c)$ and $\delta(H_c)$ are thought to have well defined *finite* values. Consequently, one expects neither a BCS relation between the lowest gap $\Delta_-(H)$ and $T_{\mathrm{SP}}(H)$, nor a simple relation between $\Delta_-(H)$ and $\delta(H)$. On the contrary, $\delta(H)$ and $T_{\mathrm{SP}}(H)$ appear more or less decoupled from $\Delta_-(H)$.

On the experimental side, there exists a relatively small number of compounds displaying properties typical of a SP system. Until recently, all available good prototypical examples of such a system were *organic* compounds like, e.g., TTF-CuBDT (Refs. 6 and 21), TTF-AuBDT (Refs. 21 and 22) or MEM(TCNQ)$_2$ (Ref. 23). For these systems, magnetic-susceptibility,[21,22,24] magnetization,[25,26] NMR (Ref. 27), x-ray,[28–30] and neutron[31] diffraction measurements were found (when performed) to agree quantitatively with most of the predictions of the standard SP theory discussed here above. Very recently,[32] the standard picture has been nicely improved by the direct observation in TTF-CuBDT of an incommensurate phase above H_c. Unfortunately, no accurate inelastic-neutron-scattering (INS) experiments could be performed on these compounds because of lack of large deuterated single crystals, so that neither the spin-gap nor the soft-phonon mode associated with the transition could be directly observed. The recent observation of a quite intriguing susceptibility in $CuGeO_3$ below 14 K strongly suggested that this germanate could be the first *inorganic* prototypical example of an SP system.[33] Since the pioneering work of

Hase and co-workers,[33,34] very comprehensive studies have been undertaken on $CuGeO_3$ by various groups, including, e.g., susceptibility,[33] magnetization,[34] neutron-scattering,[35–38] NMR (Refs. 39 and 40), electron-spin-resonance (ESR) (Ref. 41), specific heat,[42,43] Raman,[44] x-ray,[45] and electron-diffraction[46] measurements. In general, the measurements below $T_{SP}\approx 14.3$ K were found to agree more than qualitatively with most of the predictions reported so far for an SP system: exponential decay of the susceptibility at low temperature,[33,45] nonmagnetic singlet ground state,[35,39] spin-gap $\Delta\approx 24$ K in the excitation spectrum[35,36] (verifying the relation $2\Delta\approx 3.4kT_{SP}$), critical field $H_c\approx 125$ kOe above which a finite magnetization is recovered[34,41] (verifying the relation $g\mu_B H_c\approx 0.83\Delta$), existence of nuclear superlattice peaks below T_{SP} described by a commensurate propagation vector[45,46,37] $\mathbf{k}_{SP}=(1/2,0,1/2)$. However, if the SP state seems relatively well understood, a quantitative agreement with the simple picture is far from being realized above T_{SP} in the ''normal state.'' Thus, in $CuGeO_3$ the magnetic susceptibility above T_{SP} deviates strongly from the Bonner-Fisher law expected for an ideal $S=1/2$ Heisenberg chain.[47,33] Also puzzling and unconventional are the anisotropic (quasi-1D) pretransitional structural fluctuations unambiguously observed by x-ray diffraction[45] well above T_{SP}, but not seen in the neutron-diffraction experiments,[45,36,37] even in the vicinity of T_{SP}. These features have been qualitatively interpreted as a signature that the structural transition in $CuGeO_3$ was effectively triggered by the 1D-AF fluctuations, in a manner similar to some other organic compounds[30] like, e.g., $(BCP\text{-}TTF)_2X$ (where $X=PF_6$, AsF_6). Such a behavior contrasts sharply with what has been obtained in, e.g., TTF-CuBDT or $MEM(TCNQ)_2$, compounds for which both a Bonner-Fisher law and *quasi-isotropic* structural fluctuations have been observed.[6,22,30] Clearly, a more quantitative understanding of the spin-Peierls problem would require going beyond the mean-field approximation and taking into account the structural fluctuations. In $CuGeO_3$, one may expect the strongly anisotropic structural fluctuations to induce a spin pairing at very short range and, eventually, a *pseudogap* (i.e., a damped excitation at finite energy) should be present above T_{SP} in the magnetic excitation spectrum.[45] Concerning the latter point, contradictory results have been reported in the literature for $CuGeO_3$ (see Refs. 35 and 36), although a clear non-BCS behavior versus temperature has been observed below T_{SP} in all cases.

In order to further the microscopic understanding of the mechanism and the nature of the transition observed at 14 K in $CuGeO_3$, we have undertaken an exhaustive inelastic-neutron-scattering study of this compound as a function of temperature, both in zero field and under a magnetic field applied perpendicular to the chain axis. In this paper, we will focus on the evolution of both the spin dynamics and the lattice distortion with temperature and field, our main goal being to bring new pieces of information on the magneto-elastic couplings at the origin of the unconventional properties observed in this very promising compound.

The paper is organized as follows: after a brief description of the experimental conditions in Sec. II, Sec. III presents the main experimental results obtained in zero field. Section IV will be devoted to the description of field effects on the spin dynamics and the lattice distortion. Finally, we will give some conclusions and perspectives in Sec. V.

II. EXPERIMENTS

The compound $CuGeO_3$ crystallizes[48] in an orthorhombic structure of space group Pbmm, with two chemical formulas per elementary unit cell ($Z=2$) and with cell parameters $a=4.79$ Å, $b=8.425$ Å, and $c=2.94$ Å at 1.5 K. The crystallographic structure[48] can be described as a stacking of CuO_2 and GeO_4 infinite chains running along the c axis. The $S=1/2$ Cu^{2+} ions are located at the center of edge-sharing squares of oxygen atoms. Intrachain couplings between first neighbors are propagated through weakly covalent Cu-O-Cu exchange paths, whereas the magnetic chains are separated by rigid distorted GeO_4 tetrahedrons along the b axis (exchange path Cu-O-Ge-O-Cu) and the a axis (exchange path Cu-O-O-Cu). From a qualitative analysis of exchange paths, one may anticipate antiferromagnetic couplings along the b and c directions, the strength of the coupling along a being very likely much smaller than those along b and c.

The single crystals of $CuGeO_3$ used in our neutron-scattering studies were grown at LCS/Orsay using a floating-zone method associated with an image furnace. The experimental details of crystal growth have been given elsewhere (see Refs. 49 and 50). Two different samples of good quality have been prepared: one for measurements in zero field (shaped approximately as a cylinder of diameter $\phi\approx 4$ mm and length $L\approx 30$ mm), the second for studies under field (with dimensions $8\times 6\times 4$ mm^3). In the zero-field experiments, the sample was mounted in various ILL-type cryostats and oriented in all cases with the c (chain) axis lying in the equatorial plane. The cryostat was tilted in such a manner as to survey successively the $(\mathbf{b}^*,\mathbf{c}^*)$, $(\mathbf{a}^*+6\mathbf{b}^*,\mathbf{c}^*)$,$(\mathbf{a}^*+10\mathbf{b}^*,\mathbf{c}^*)$ scattering planes. In the experiments with an applied field, the sample was aligned with the plane $(\mathbf{a}^*+6\mathbf{b}^*,\mathbf{c}^*)$ in the equatorial plane and mounted in a 10-T vertical field cryomagnet. The neutron-scattering experiments were performed on various three-axis spectrometers: DN1, installed on a thermal beam at the Siloë reactor of CEN-Grenoble; and 1T, installed on a thermal beam at the Orphée reactor of LLB/CEN-Saclay. Different configurations have been used. On DN1, the incident wave vector k_i was held fixed at 2.62 Å^{-1} and both the (002) pyrolithic graphite (PG) monochromator and analyzer were vertically focused. We have used horizontal collimations 25′-30′-S-60′-30′ (experiments in zero field) or 25′-30′-S-60′-60′ (experiments under field), yielding a resolution in energy of about 0.6 and 0.74 meV, respectively. On 1T the final wave vector k_f was held fixed at 2.662 Å^{-1}, with a vertically focusing PG(002) monochromator and a horizontally focusing PG(002) analyzer. With such a configuration, the resolution amounted to about 1 meV. Some neutron-diffraction experiments have been performed on the two-axis spectrometer DN3 equipped with a lifting arm detector, installed at the Siloë reactor. In these measurements, the incident wave length was fixed at 1.53 Å, produced by a PG(002) monochromator. The sample was mounted in the 10-T cryomagnet and oriented with the $(\mathbf{a}^*+6\mathbf{b}^*,\mathbf{c}^*)$ plane horizontal, allowing to observe nonequatorial reflections between $-5°$ and 12°.

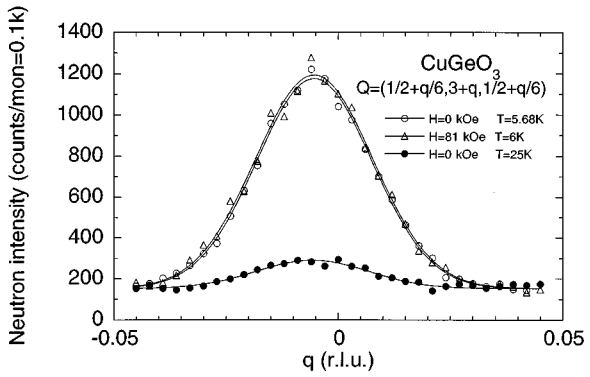

FIG. 1. Longitudinal elastic scans across the (1/2,3,1/2) superlattice peak at zero field [$T=5.68$ K (○) and $T=25$ K (●)] and at $H=81$ kOe [$T=6$ K (△)]. The solid lines are fits to Gaussian functions as described in the text.

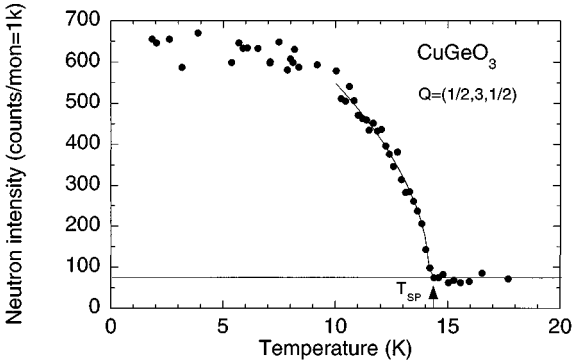

FIG. 2. Temperature dependence of the neutron intensity at point (1/2,3,1/2), showing the disappearance of the lattice distortion at $T_{SP}=14.2$ K. The solid line is a fit to a power law, as described in the text.

III. NEUTRON SCATTERING IN ZERO FIELD

In $CuGeO_3$, the first problem considered has been to try to detect the presence of superlattice peaks arising either from a hypothetical lattice dimerization or from the existence at low temperature of a long-range (3D) magnetic ordering. Powder-diffraction experiments performed on the three-axis spectrometer DN1 have shown *no trace* of additional superlattice peaks in the diffraction patterns, at least down to 1.7 K. This negative result implies the lack of long-range magnetic ordering well below 14 K, the temperature at which $\chi(T)$ starts to drop rapidly.[33] The disappearance of magnetic fluctuations at low temperature and low energy, a signature of a nonmagnetic singlet ground state, has been unambiguously observed from NQR measurements of the spin-lattice relaxation time T_1 as a function of temperature.[39] Between 5 and 13 K, the fluctuation rate $T_1^{-1}(T)$ has been found to vanish rapidly with T, following closely an exponential law $T_1^{-1}(T)\propto T\exp(-\Delta/kT)$, with a gap value $\Delta\approx 20-25$ K. Recent NMR measurements[51] performed below 5 K have confirmed these results, showing that at very low temperature $1/T_1\propto\exp(-2\Delta/kT)$ with $\Delta\approx 24$ K, in agreement with the theoretical prediction for an SP system.[52] As we shall see later, the absence of 3D magnetic ordering in $CuGeO_3$ is a direct consequence of the small value of the correlation length, despite the existence of relatively large interchain couplings in this compound. We will come back to this point more quantitatively in Sec. III C. In what concerns the dimerization itself, the powder data only indicate that the intensity of superlattice peaks must be very weak, implying a rather small lattice distortion (remember that qualitatively $I_D(\mathbf{Q})\propto(\langle\delta\rangle_T)^2$, where $\mathbf{Q}$ is the scattering vector associated with the superlattice peak). Accurate neutron-diffraction measurements on *single crystals* have confirmed the lack of 3D magnetic order down to 1.4 K, but have allowed a clear observation of the lattice distortion in $CuGeO_3$.

A. Lattice distortion in $CuGeO_3$

The first evidence of the existence of superlattice peaks below T_{SP} in $CuGeO_3$ was obtained from x-ray diffraction[45] and electron-scattering[46] measurements. The observed satellites were indexed with a commensurate propagation vector $\mathbf{k}_{SP}=(1/2,1,1/2)$, corresponding to out-of-phase motions from the initial atomic positions. Neutron-diffraction measurements on single crystals have confirmed the presence of nuclear satellites not only at scattering vectors $\mathbf{Q}=(1/2,2n+1,1/2)$ (Refs. 45, 36, and 37) but also at $\mathbf{Q}=(1/2,2n,1/2)$ (Ref. 37), a fact which indicates that the propagation vector is more rigorously $\mathbf{k}_{SP}=(1/2,0,1/2)$. Figure 1 shows a typical longitudinal scan across the satellite (1/2,3,1/2) performed on the DN1 spectrometer at a temperature of about 6 K. Clearly, a well-defined peak is observed, with a q width only limited by the instrumental resolution. This implies a true long-range ordering for the lattice distortion. Very similar results have been obtained at peak positions (1/2,5,1/2), (1/2,1,3/2), and (1/2,3,3/2), which confirm the propagation vector $\mathbf{k}_{SP}$ previously determined. Table I summarizes the corresponding integrated intensities obtained from ω scans performed on the DN3 two-axis spectrometer, following standard experimental

TABLE I. Observed structure factors (arbitrary units) for some dimerization superlattice peaks at zero field and 98 kOe. For comparison, we have also given rescaled values obtained by the BNL group (after Ref. 37).

Q	I_DL $T=5$ K $H=0$	I_DL $T=5$ K $H=98$ kOe	I_DL (scaling from Ref. 37)
(−1/2,3,−1/2)	5.5±0.3	5.4±0.3	5.5
(−1/2,5,−1/2)	6.6±0.4	6.0±0.4	7.8
(1/2,−1,3/2)	4.6±0.3	4.8±0.3	
(−1/2,3,3/2)	0.3±0.15	0.3±0.15	0.2
(0,0,1)	4830±100	4980±100	

procedures. These data have been corrected by the Lorentz factor $L(\mathbf{Q})$ and by second-order contamination, the latter contribution being determined for each position by performing the same ω scans at 23 K. The purely nuclear nature of these peaks has been unambiguously established from their dependencies of both the scattering vector $\mathbf{Q}$ and the temperature. Figure 2 shows, for example, the temperature dependence of the satellite (1/2,3,1/2). As can be seen, the peak intensity vanishes at about 14.2 K, a temperature which can be taken as an accurate estimate of T_{SP}.

We have analyzed our experimental results in the vicinity of T_{SP} starting from a conventional power-law behavior given by the relation $I_D(T)=I_{BG}+I_D(0).(1-T/T_{SP})^{2\beta}$, where I_{BG} is the residual background intensity determined above T_{SP} and β is a pseudoexponent characterizing the nature of the transition. The best fit to our data is achieved with parameters $I_{BG}=74$, $I_D(0)=895\pm20$, $T_{SP}=14.2\pm0.2$ K, and $\beta=0.26\pm0.03$. In particular the latter value is far from corresponding to the expected mean-field value $\beta=0.5$, in agreement with previous x-ray[53] and neutron-diffraction[36] measurements. This small value of β is consistent with the existence in $CuGeO_3$ of strongly anisotropic critical fluctuations, observed in this material by Pouget *et al.*[45] by x-ray diffraction. However we emphasize that no such fluctuations have been detected in the present neutron-diffraction experiments, as can be easily seen in Fig. 2. We will discuss this point later. An alternative explanation for the small β has been proposed, which would bring into play the proximity of a tricritical point.[53]

From the observed intensities, we have found a ratio of the order of 10^{-3} between the strongest dimerization-peak intensities and the (0,0,1) nuclear Bragg-peak intensity. This small ratio confirms quantitatively the smallness of the atomic displacements in $CuGeO_3$ and explains quite well the difficulty to observe satellites in neutron-scattering measurements performed on *powdered* samples. An accurate neutron scattering study of satellite intensities has been undertaken by Hirota *et al.*,[37] and has allowed a quantitative determination of the various atomic displacement vectors $\boldsymbol{\delta}_j$ at low temperature. According to their model, the main atomic shifts are observed for the Cu atoms along the c axis and O(2) atoms in the ($\mathbf{a}$,$\mathbf{b}$) basal plane, with very small relative atomic displacements values $\delta^c_{Cu}/c\approx0.0022$, $\delta^a_O/a\approx0.0018$, and $\delta^b_O/b\approx0.0013$. Table I gives a comparison between the present data and the corresponding data obtained in Ref. 37. As can be seen, our data appear quantitatively consistent with those of Ref. 37 and, consequently, confirm the proposed structure. For a quantitative analysis we have used the following expression for the integrated intensity of a superlattice peak defined by the scattering vector $\mathbf{Q}=\mathbf{H_N}+\mathbf{k}_{SP}$:

$$I_D(\mathbf{Q})L(\mathbf{Q})\propto\left|\sum_j\ (2\pi\mathbf{Q}\cdot\boldsymbol{\delta}_j)b_j\ \exp(2\pi i\mathbf{Q}\mathbf{R}_j)\right|^2,$$

where $\mathbf{H_N}$ is a vector of the reciprocal space, $L(\mathbf{Q})$ is the Lorentz factor, $\boldsymbol{\delta}_j$ is the thermal average displacement of atom j, b_j being its associated scattering length, and $\mathbf{R}_j$ its position in the undistorted elementary unit cell. The normal nuclear-Bragg-peak intensities have been analyzed from the well-known relation:

$$I_N(\mathbf{H}_N)L(\mathbf{H}_N)\propto\left|\sum_j\ b_j\ \exp(2\pi i\mathbf{H}_N\mathbf{R}_j)\right|^2.$$

Assuming that the model proposed in Ref. 37 is valid and neglecting in our analysis all extinction or absorption corrections, it has been possible from our data to deduce values for the displacements of Cu atoms along the c axis and O(2) atoms along the b axis. We have obtained the following reduced values, using scattering lengths $b_{Cu}=0.77$, $b_{Ge}=0.82$, and $b_O=0.58\times10^{-12}$ cm: $\delta^c_{Cu}/c\approx0.0028$ and $\delta^b_O/b\approx0.0013$, the component δ^a_O being determined with low accuracy from the present data. The main reason for this is the impossibility of having access to scattering vectors with higher Q_a components (3/2,5/2,...), due to the use of a cryomagnet that has strongly limited the observable vertical angular window. The displacements obtained from the present determination are in quantitative agreement with previous estimates. Since magnetic interactions along the chain axis involve mainly superexchange through O(2) oxygen atoms, the Cu and O(2) shifts are expected to induce alternating exchange in the system, due to nonsymmetric modifications in the Cu-O(2)-Cu geometry. This will have important consequences on the magnetic excitation spectrum, as we will see in Sec. III B.

No trace of quasielastic pretransitional structural fluctuations could be detected in our neutron-scattering experiments performed on the three-axis spectrometers DN1 and 1T, at scattering vector $\mathbf{Q}=(1/2,3,1/2)$. This fact is illustrated in Fig. 2, e.g., where no tail is observed in the neutron-scattering intensity above T_{SP}. Our data suggest for the magnitude of the structural fluctuations a value at least 10^2 times smaller than the value observed for a dimerization peak. Negative results were also obtained in the vicinity of T_{SP} at higher scattering vectors, e.g., $\mathbf{Q}=(1/2,5,1/2)$, using the DN1 spectrometer set in the two-axis configuration (i.e., analyzer removed). With such a configuration, one expects to integrate, at least partially, over a wider energy range limited only by the neutron incident energy ($E_i\approx14$ meV in our case). The fact that *no nonmagnetic* signal could be detected above T_{SP} in the quasi-elastic-neutron-scattering experiments strongly suggests that the structural response, if sizable, is very likely inelastic or broad in energy. In fact the structural fluctuations are probably also *very small* in amplitude and, anyway, always superimposed on the magnetic fluctuations. This renders their observation very difficult by neutron diffraction, in contrast with x-ray diffraction, a technique that integrates over the full energy spectrum and, moreover, is very weakly sensitive to magnetism.

For the same reasons, and despite very careful measurements,[56] it has not been possible to observe any phonon softening at T_{SP}. These negative results, also reported by Lorenzo *et al.*,[38] Nishi, Fujita, and Akimitsu[54] and Hirota *et al.*[55] may be attributed either to the weakness of the relevant phonon or to the nature of the phase transition itself, which could be of order-disorder type and not at all of displacive type as expected in the standard theory. In this case, additional phonon branches should be present at low temperature around $\mathbf{q}=\mathbf{k}_{SP}$. A rough estimate of the expected counting rate for these ''dimerized'' phonons can be made. Typical phonon measurements in $CuGeO_3$ give counting rates of the order of 100 neutrons per minute at low tempera-

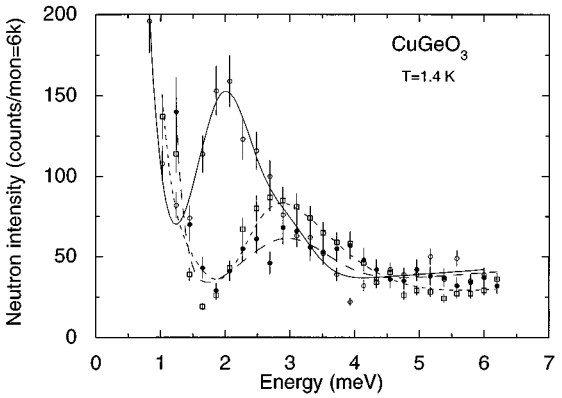

FIG. 3. Constant-Q scans at different scattering vectors $\mathbf{Q}=(0,1,3/2)$ (○), $\mathbf{Q}=(1/2,3,1/2)$ (□) and $\mathbf{Q}=(1/2,5,1/2)$ (●), showing the dispersion of magnetic excitations along the a^* direction perpendicular to the chain axis. Solid lines are guides for the eye.

ture. Taking into account the 10^{-3} ratio observed between the dimerization peaks and the normal Bragg peaks, one expects a phonon intensity of the order of 0.1 n/min. This phonon contribution should be superimposed on a background contribution of the order of 0.5−1 n/min and to the inelastic magnetic contribution, which amounts at the scattering vector $\mathbf{Q}=(1/2,5,1/2)$ to about 10 n/min (as will be seen in the next section). Therefore, the main difficulty is to eliminate the magnetic contribution, always present and superimposed on the lattice contribution. In our opinion this will not be trivial, even using polarized neutrons and full polarization analysis.

B. Spin dynamics in $CuGeO_3$

As mentioned in Sec. I, the SP ground state is expected to be a nonmagnetic singlet ground state well separated from the first excited triplet state by an energy gap of magnitude $\Delta\approx 1.76kT_{SP}\approx 2.1$ meV≈ 25 K. Macroscopic data from measurements such as susceptibility,[33] magnetization,[34] or specific heat[42] have given strong evidence for the existence of such a gap in $CuGeO_3$. This gap has been further confirmed by more microscopic techniques like, e.g., NMR (Ref. 39) or ESR (Ref. 41), which have provided for Δ a value of the order of 24 K.

In order to determine directly the magnetic excitation spectrum, INS experiments have been performed on single crystals of $CuGeO_3$. We have measured the dispersion relation of the magnetic excitations both along the chain direction and perpendicular to it (both along $\mathbf{a}^*$ and $\mathbf{b}^*$). In these studies, the first problem was to determine the *antiferromagnetic wave vector* $\mathbf{k}_{AF}$ at which the magnetic excitation spectrum displays its minimum in energy. Obviously one must have $k^z_{AF}=1/2$ for the component along the c^* axis, owing to the AF intrachain coupling. From a qualitative analysis of interchain couplings along the b axis, which involves Cu-O-Ge-O-Cu bonds, one may also anticipate an antiferromagnetic coupling. Taking into account the fact that there are two Cu atoms per unit cell along the b direction, one expects a component $k^y_{AF}=1$ along the b^* axis. The third component k^x_{AF} was determined directly by measuring the dispersion relation along a^*. Figure 3 shows scans in energy performed on the 1T spectrometer at a temperature of $T=1.4$ K, well below the characteristic temperature Δ/k, for three values of the scattering vector: $\mathbf{Q}=(0,1,3/2)$, $(1/2,3,1/2)$, and $(1/2,5,-1/2)$, located at the center (for the former) and at the boundary (for the two latter) of the Brillouin zone. The former scan exhibits a sharp maximum at 2 meV, whereas the two latter exhibit a broader maximum at a slightly higher energy of about 2.7 meV. Table II gives a comparison between the peak position, the energy-integrated intensity and the energy width [full width at half maximum (FWHM)] of the three observed modes. The Q dependence of the intensity shows that the observed excitations are of magnetic origin. The shift in peak position clearly reveals the existence of a sizable dispersion along the a^* axis (perpendicular to the chain axis), with a minimum in energy observed at points corresponding to the wave vector $\mathbf{k}_{AF}=(0,1,1/2)$. We note (without explanation so far) that the antiferromagnetic wave vector $\mathbf{k}_{AF}$ and the propagation vector of the lattice distortion $\mathbf{k}_{SP}=(1/2,0,1/2)$ differ by their components perpendicular to the chain axis. Obviously, the dispersion along a^* must be attributed to the existence of a weak *ferromagnetic* coupling along the a direction. We will come back to a more quantitative analysis of these data below.

TABLE II. Evolution of the peak position (ω_M), peak amplitude (I_M) and full width at half maximum ($\Delta\omega$) of the magnetic response at $\mathbf{q}=\mathbf{k}_{AF}$, as a function of the scattering vector $\mathbf{Q}$.

$\mathbf{Q}$	ω_M (meV)	I_M (counts/mon=6k)	$\Delta\omega$ (meV)
(0,1,1/2)	2.0±0.05	360	1
(0,1,3/2)	2.0±0.05	120	1
(1/2,3,1/2)	2.7±0.1	30	1.5
(1/2,5,−1/2)	2.8±0.1	20	1.5

Quite surprisingly, an even more pronounced dispersion was observed along the b^* direction, also perpendicular to the chain axis. Figure 4 shows typical scans in energy performed on the DN1 spectrometer, at $T=1.8$ K, for three values of the scattering vector $\mathbf{Q}=(0,-1+q_b,1/2)$, with $q_b=0$, 0.4, and 0.8. The pronounced dispersion was observed along the b^* direction, which confirms the rather poor 1D character of $CuGeO_3$. This fact, first reported by Nishi, Fujita, and Akimitsu[35] is now well established by several independent

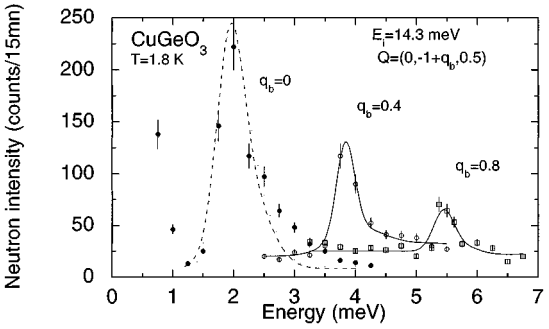

FIG. 4. Constant-Q scans at different scattering vectors $\mathbf{Q}=(0,-1+q_b,1/2)$ with $q_b=0$ (●), 0.4 (○), and 0.8 (□), showing the dispersion of magnetic excitations along the b^* direction, also perpendicular to the chain axis. The solid lines are guides for the eye.

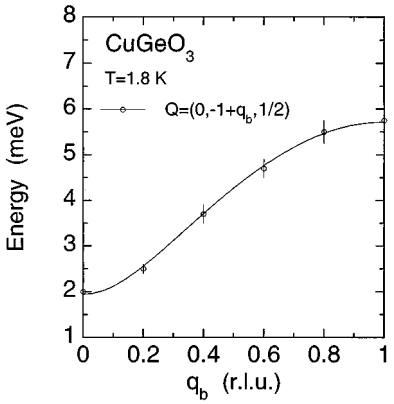

FIG. 5. Dispersion of the magnetic excitations along b at 1.8 K. The open symbols are the experimental data. The solid line is a fit to Eq. (7).

measurements.[36,41] Figure 5 represents the dispersion relation which was obtained along b^*. The minima in energy are observed for components $q_b=0,2,...$ at about 2 meV, while the maxima in energy occur at components $q_b=1,3,...$ at about 5.8 meV. As previously mentioned, such a dispersion reveals the existence of relatively strong *antiferromagnetic* couplings along the b axis. We will discuss later the quantitative analysis of these experimental results.

More important, we have attributed the energy minimum at $\mathbf{q}=\mathbf{k}_{\mathrm{AF}}$ to the existence of an *energy gap* $\Delta\approx 2$ meV≈ 23 K in the excitation spectrum. The ratio $2\Delta/kT_{\mathrm{SP}}\approx 3.32$, although slightly smaller, is found to obey closely the BCS relation, as predicted theoretically for an SP system (see Sec. I). This value is also in good quantitative agreement with previous INS (Refs. 35 and 36) and indirect[39,41,42] determinations.

Further information was obtained by measuring the dispersion relation and the intensities of magnetic excitations along the chain axis. Figures 6(a) and 6(b) show several magnon groups observed with the 1T thermal neutron spectrometer, which give evidence for a strong dispersion along c^*. Figure 7 shows the evolution of three scans in energy performed in the vicinity of $q=0$, at scattering vectors $\mathbf{Q}=(0,1,1+q)$ with $q=0.15$, 0.05, and 0. We have determined the mode energy for each q value as being the position at maximum intensity, neglecting in a first approximation all resolution or intensity corrections. Following this procedure, we deduced the dispersion curve of magnetic excitations along the c^* direction, shown in Fig. 8, for reduced wave vectors $q_c=1/2-q$ covering the first Brillouin zone. Within experimental error bars, the excitation spectrum is found to be *quasisymmetric* with respect to $q_c=1/4$, where it displays its maximum in energy at $\omega_M\approx 15.7$ meV. Obviously, this last quantity must reflect directly the strength of the intrachain couplings.

As previously discussed in Sec. III A, the dimerization of Cu atoms below T_{SP} induces alternating exchange and the *ideal* magnetic system at low temperature is expected to be reasonably well described by an alternating-chain Hamiltonian (1). Taking into account the finite interchain couplings observed experimentally in the *real* system, a more appropriate Hamiltonian describing the magnetic properties of $CuGeO_3$ could be written as

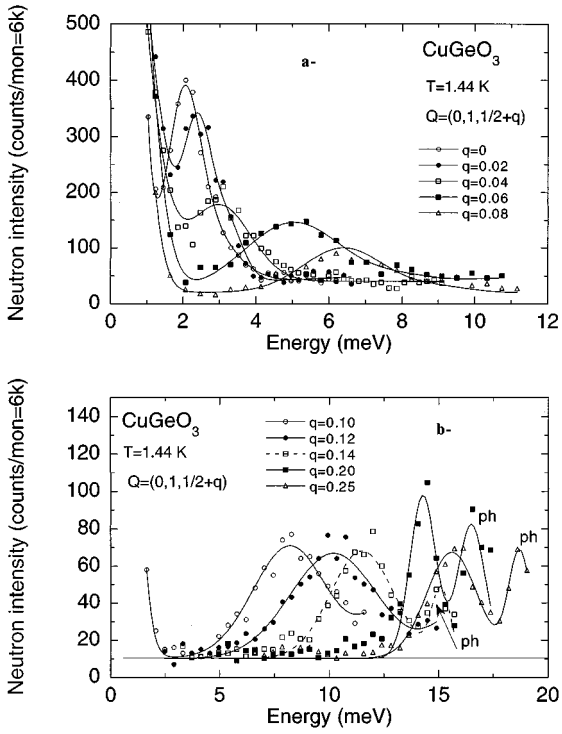

FIG. 6. Constant-Q scans at scattering vectors $\mathbf{Q}=(0,1,1/2+q)$ for a temperature $T=1.44$ K, showing the dispersion along the chain axis: (a) $q=0$, 0.02, 0.04, 0.06, and 0.08; (b) $q=0.1$, 0.12, 0.14, 0.20, and 0.25. The solid lines are guides for the eye.

$$H=2J_1\sum_i\left(\mathbf{S}_{2i}\cdot\mathbf{S}_{2i+1}+\alpha\mathbf{S}_{2i+1}\cdot\mathbf{S}_{2i+2}\right)+J'_a\sum_{i,j}\mathbf{S}_i\cdot\mathbf{S}_j$$

$$+J'_b\sum_{i,j}\mathbf{S}_i\cdot\mathbf{S}_j\,, \tag{5}$$

in which J'_a and J'_b are the interchain coupling constants along a and b, respectively. In relation (5), the subscript j numbers spins belonging to adjacent chains. Unfortunately, there are *no* precise quantum calculations giving the dispersion relation corresponding to Hamiltonian (5) with finite J'_a and J'_b. In a first approximation, order of magnitude estimates for J_1 and α can be obtained by assuming $J'_a\approx J'_b\approx 0$. In this case, theoretical calculations are available for the

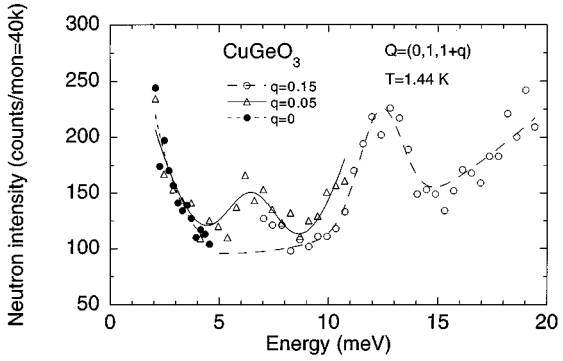

FIG. 7. Constant-Q scans at scattering vectors $\mathbf{Q}=(0,1,1+q)$ with $q=0.15$, 0.05, and 0 showing the energy dependence of the magnetic excitations as $q\to 0$. The lines are guides to the eye.

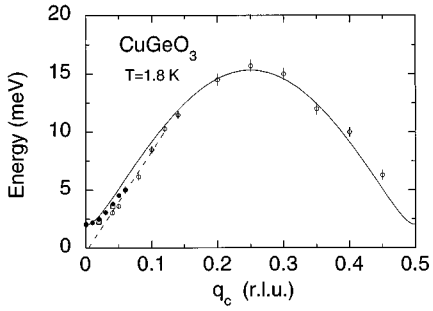

FIG. 8. Dispersion curve of the magnetic excitations at 1.8 K for wave vectors directed along the chain axis. The solid line is a fit to the theoretical dispersion relation as given by Eq. (6). The dashed line corresponds to the linear relation $\omega(q_c)\approx c_0 q_c$.

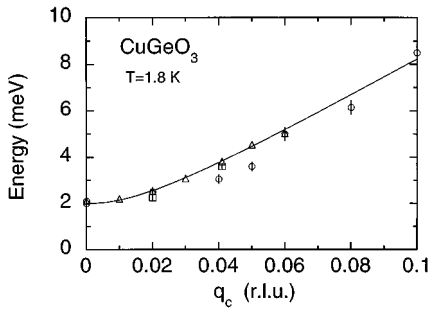

FIG. 9. Dispersion relation along the chain at small reduced wave vectors $q_c=q-1/2$. The open symbols are the experimental data obtained on various three-axis spectrometers [(○) 1T, (△) DN1, and (□) 4F1]. The solid line is a fit to the relation: $\omega(q_c)\approx(\Delta^2+c_0^2 q_c^2)^{1/2}$, as explained in the text.

spin-1/2 alternating chain.[9] As for the uniform chain, a continuum of triplet excited states is expected to exist above a lower limit $\omega_1(q_c)$ given approximately by the relation[9]

$$\omega_1(q_c)\approx\sqrt{\Delta^2+(\omega_M^2-\Delta^2)\sin^2(2\pi q_c)}, \tag{6}$$

where Δ and ω_M have been previously defined and where the reduced wave vector $q_c=1/2-q$ is expressed in reciprocal lattice unit (r.l.u.). Both Δ and ω_M are functions of the exchange parameters J_1 and α. For the ideal 1D case, we have[9] $\omega_M\approx\pi J_1[(1+\alpha)/2]$, while the energy gap $\Delta(J_1,\alpha)$ is calculated numerically.[9–13] A recent determination[13] gave $\Delta(J_1,\alpha)\approx 1.05(2J_1)(1-\alpha)^{2/3}$. Quite similar to the case of the spin-1/2 uniform chain, the dynamic structure factor $S(q_c,\omega)$ is expected to display a maximum at an energy $\omega(q_c)$, located only slightly above $\omega_1(q_c)$; the latter quantity reflecting with a sufficiently good accuracy the pseudodispersion relation of the magnetic excitations. In other words the experimental data can be analyzed directly from Eq. (6). The solid line in Fig. 8 is calculated from Eq. (6), using the experimental values of Δ and ω_M. These values are obtained self-consistently using the exchange parameters $(2J_1)\approx 10.5$ meV$\approx$122 K and $\alpha\approx 0.92$. The present determination of $2J_1$ is in good agreement with a previous INS determination by Nishi, Fujita, and Akimitsu[35] based on an anisotropic antiferromagnetic model. However, our value of α is found significantly larger: 0.92 in the present analysis instead of 0.78 in Ref. 35, indicating a much weaker alternation. The reason for this discrepancy arises mainly from the use of the Pytte's mean-field expression[5] $\Delta\approx 1.64(2J)\,\delta$ in Ref. 35, which differs by almost a factor of 2 from the numerical determination of $\Delta(J_1,\alpha)$. From our determination, we obtained a lattice-distortion parameter $\delta=(1-\alpha)/(1+\alpha)\approx 0.042$, which is qualitatively consistent with the relatively small amplitude of the atomic displacements observed by neutron diffraction[37] (remember that $\delta_{\mathrm{Cu}}\approx 0.007$ Å).

As can be seen in Fig. 8, the agreement between the theoretical curve (solid line) and our INS data is far from perfect. There are at least four reasons for this. First, expression (6) is only an approximation which may not reproduce accurately the maximum of $S(q_c,\omega)$ if the continuum is too strong. Secondly, the poor 1D character of $CuGeO_3$ is expected to modify appreciably the ideal dispersion relation given by the simple Eq. (6). We will come back to this point later. Thirdly, next-nearest-neighbor (NNN) intrachain couplings[68] could play a role going against the 3D interchain couplings and favor quantum disorder. Indeed, theoretical calculations[57–59] have clearly demonstrated the tendency to spontaneous dimerization when the ratio of NNN to NN intrachain coupling constants is larger than 1/4. Unfortunately, the dispersion relation of magnetic excitations is unknown for that model, which strongly limits a more quantitative analysis. The last reason is a purely experimental one: finite resolution corrections could play a non-negligible role, especially in experiments in which horizontal focusing devices (monochromator and analyzer) have been used. This is clearly illustrated in Fig. 9, which compares our experimental data at low q_c from different spectrometers: thermal 1T [open circles, $\mathbf{Q}=(0,1,1/2+q_c)$], cold 4F1 [open squares, $\mathbf{Q}=(0,1,1/2+q_c)$], and thermal DN1 [open triangles, $\mathbf{Q}=(0,1,1/2-q_c)$]. Due to a better instrumental resolution in both wave vector and energy and better focusing conditions with respect to the dispersion curve, the data obtained at low q_c on the last two spectrometers give slightly larger energies. Moreover, they appear much closer to the theoretical prediction $\omega(q_c)\approx\sqrt{\Delta^2+(c_0 q_c)^2}$ than those obtained on the 1T spectrometer. In Fig. 9, the solid line is calculated from the relation above with a spin-wave velocity $c_0\approx 80$ meV/r.l.u.$\approx$38 meV Å. This value is found to be 20% smaller than the theoretical prediction $\sqrt{\omega_M^2-\Delta^2}d\approx 96$ meV/r.l.u.$\approx$45 meV Å expected for the simple alternating-exchange Hamiltonian. The dashed line in Fig. 8 represents the classical behavior $\omega(q_c)\approx c_0 q_c$ calculated with $c_0\approx 40$ meV Å, which accounts for the experimental data down to $\tilde{q}_c\approx 0.05$ r.l.u. Below this value, $\omega(q_c)$ deviates rapidly from a linear relation, as an effect of the opening of the gap. We will see later that $1/\tilde{q}_c\approx 10$ Å reflects roughly the value of the intrachain correlation length. We believe that the remaining difference of about 20% observed between the experimental and the calculated dispersion law at low q_c is a sign that the Hamiltonian (1) is much too "simple" to describe the reality. As discussed above, a possible improvement could result from the introduction of interchain coupling constants J_a' and J_b' or, possibly, by taking into account the NNN intrachain exchange couplings.

Although no precise theory exists to date, rough estimates of the magnitude of the interchain couplings can be obtained from antiferromagnetic spin-wave theory for an *anisotropic* system with two Bravais sublattices, the SP gap being simulated by an anisotropy gap. For the dispersion along the b^*

axis (of antiferromagnetic type), the predicted expression is the following (with q_b expressed in r.l.u.):

$$\omega(q_b) \approx \sqrt{\Delta^2 + (\Delta E)_b^2 \sin^2(\pi q_b/2)}. \quad (7)$$

In deriving relation (7), we have implicitly taken into account the fact that there are two Cu atoms in the elementary unit cell along the b axis. The solid line in Fig. 5 corresponds to the best fit of experimental data to Eq. (7) with parameters $\Delta \approx 2$ meV and $(\Delta E)_b \approx 5.3$ meV. Using the *classical* spin-wave results $(\Delta E)_b \approx 2S\sqrt{zz_b'|JJ_b'|}$ and $\omega_M \approx 2Sz|J|$, with $S=1/2$ and where $z=2$ and $z_b'=2$ are the numbers of adjacent spins along c and b, respectively, and J is the average intrachain exchange value, one deduces a ratio $|J_b'/J| \approx [(\Delta E)_b/\omega_M]^2 \approx 0.11$. This value confirms quantitatively the poor 1D character of $CuGeO_3$.

In what concerns the dispersion along the a^* direction (of ferromagnetic type), the predicted expression can be written as

$$\omega(q_a) \approx \sqrt{\Delta^2 + (\Delta E)_a^2 \sin^2(\pi q_a)}, \quad (8)$$

which fits the experimental data with a coefficient $(\Delta E)_a \approx 1.66$ meV, implying a ratio $|J_a'/J| \approx 0.011$ about 10 times smaller than for the b^* direction. Although derived in a slightly different manner, our determinations agree very quantitatively with those obtained previously by Nishi, Fujita, and Akimitsu.[35] The strong value of $|J_b'/J|$, by modifying both the quantum character (expected to be less important) and the effective dimension of the system (in fact intermediate between 1D and 2D), may bring quantitative changes in the J and J' values determined previously. Qualitatively, one expects an increase of J (and also of J_1) resulting from the fact that the coefficient relating ω_M to J is no longer $\pi \approx 3.14$, but a number slightly smaller (but larger than 2.36, the value expected for an ideal 2D Heisenberg system[60]). However, for a more quantitative determination of these parameters, a more accurate theory is needed, particularly to explain the unusual shape of $\chi(T)$.

C. Equal-time structure factor and correlation length

In all our INS measurements at $\mathbf{q}=\mathbf{k}_{AF}$, the line shape of the inelastic magnetic response at low temperature has been found to be relatively asymmetric. This fact is well documented by considering, for example, the energy scan at $q_b=0$ shown in Fig. 4, performed on the DN1 spectrometer set in the constant-E_i mode. Experimentally, the magnetic signal displays a quite visible tail on the high-energy side, which extends up to at least 5 meV within the accuracy of our measurements [remember that in the constant-E_i mode, the signal decreases rapidly at high energy, roughly as $(1-\omega/E_i)^2$]. Numerical calculations taking into account the resolution effects produced by the curvature of the dispersion relation of the magnetic excitations (which give rise to a similar tail) show that the dynamic structure factor cannot be described solely by a δ function in energy. The dashed line in Fig. 4 represents the result of such a calculation, using a 1D structure factor $S(q_c,\omega) \propto \delta[\omega - \omega(q_c)]$ convoluted with the full 4D Gaussian resolution function and corrected by the neutron normalization factor[67] $k_f^3 \cot g(\theta_a)$. Most certainly, it is impossible to reproduce quantitatively the signal observed above typically 2.5 meV. Accordingly, the unfolded $S(q_c,\omega)$ should exhibit an intrinsic tail on the high-energy side, which could originate from the continuum predicted theoretically.[9,13] Unfortunately, to our knowledge no precise analytic expression for $S(q_c,\omega)$ exists for an alternating chain system. This renders further quantitative analysis of the inelastic line shape difficult. Moreover, such an analysis requires the introduction of the 4D instrumental resolution function $R(\mathbf{Q},\omega)$, which is not a simple tool in general. To avoid all these complications, we prefer considering the neutron intensity integrated in energy over the inelastic peak, formally defined by the expression $S(q)=\int S(q,\omega)d\omega$. The integration over ω cancels the effect of the resolution in energy, assuming for $R(\mathbf{Q},\omega)$ a generalized Gaussian function. Furthermore, such a procedure presents the advantage of integrating (at least partly) over the continuum, whenever it exists in the real system. In principle, using such a procedure, one has only to consider the resolution in q, which turns out to have little effect in this problem where the physics is generally broad in q (remember that $1/\xi \approx 0.05$ r.l.u. whereas typically $\Delta_q^{Res}/2 \approx 0.01-0.02$ r.l.u.). Figure 10 summarizes the dependence of the integrated intensity as a function of the reduced wave vector along the chain. Without any surprise, $S(q)$ is maximum at $q=1/2$ and decreases continuously as $q \to 0$, to vanish completely at $q=0$. Qualitatively, two distinct behaviors are observed on both sides of 1/4: a Lorentzian-like behavior above $q=1/4$, whereas an almost linear regime seems to take place below $q=1/4$. Quantitatively, one observes an integrated intensity about 20 times smaller at $q=0.05$ than at the symmetric position $q=1/2-0.05$, which shows that the decrease of $S(q)$ with q is not so rapid. A much stronger q dependence has been observed in the spin-1 Haldane-gap system NENP.[61]

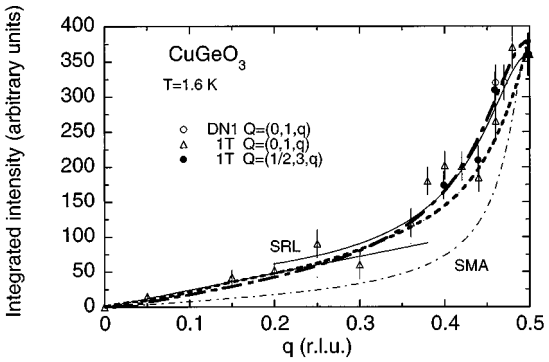

FIG. 10. Intensity integrated in energy as a function of the wave vector component along the chain. Symbols are the experimental data obtained on DN1 (●) and 1T (△,○) spectrometers. The various lines correspond to different calculations or fits as described in the text.

Due to the absence of quasielastic scattering at low temperature (resulting from the nonmagnetic singlet ground state), the correlation length ξ can be estimated from $S(q)$, which is directly related to the Fourier transform of the equal-time correlation function $\langle \mathbf{S}_0\mathbf{S}_r \rangle$. According to Okamoto,[62] this function is predicted to behave exponentially at large r values for an antiferromagnetic alternating chain, following the relation

$$\langle \mathbf{S}_0\mathbf{S}_r \rangle \propto (-)^r \exp(-r/\xi)/\sqrt{r/\xi}. \quad (9)$$

By taking the Fourier transform of Eq. (9), one derives easily a square-root Lorentzian (SRL) expression for $S(q)$:

$$S(q) \propto \xi / \sqrt{1+(q-k_{\mathrm{AF}})^2 \xi^2} \tag{10}$$

where $k_{\mathrm{AF}}=\pi/c$ and q are expressed in Å^{-1}. In principle, relation (10) is only valid for small values of the argument $q-k_{\mathrm{AF}}$. The solid line in Fig. 10 represents the best fit of experimental data to the SRL function, giving a correlation length of $\xi \approx 9$ Å, which corresponds approximately to three intrachain spacing distances ($\xi/c \approx 3$). Experimentally, one finds that Δ and ξ follow quantitatively the relation $2\Delta \approx c_0/\xi$, and not the relation $\Delta \approx c_0/\xi$ as predicted, for example, for the spin-1 isotropic chain[63] (see also Ref. 62). A more accurate and general expression for $S(q)$ can be deduced from an exact sum rule valid only in one dimension.[64] Quite generally, $S(q)$ can be written in the form: $S(q) \propto [1-\cos(2\pi q d)]/\langle \omega_q \rangle$, where we have introduced the average energy $\langle \omega_q \rangle = \int S(q,\omega)\omega d\omega / \int S(q,\omega) d\omega$. If the spectral function $S(q,\omega)$ is not too far from a δ function in energy [i.e., assuming $S(q,\omega) \approx S(q)\delta(\omega-\omega(q))$], then one should have $\langle \omega_q \rangle \approx \omega(q) \propto \sqrt{1+(\omega_M/\Delta)^2 \sin^2(qd)}$ (with a ratio $\omega_M/\Delta \approx 7.8$ in the present case). The plain dot-dashed line in Fig. 10 is calculated using the above relation, which in fact corresponds to the so-called ''single-mode approximation'' (SMA). Without any ambiguity, the SMA is unable to reproduce the experimental data in the full range of q values. However, our experimental data at low q (i.e., roughly for $0.05<q<0.2$) are quite compatible with the low-q SMA expression $S(q) \propto q^2/\sqrt{1+(c_0/\Delta)^2 q^2}$, which predicts a *linear* behavior as soon as $q > 2\Delta/c_0 \approx 0.05$ r.l.u. Unfortunately, the partial agreement obtained at low q inevitably increases the disagreement around the antiferromagnetic point, the SMA predicting a signal roughly 2.5 times larger than the observed one. A much better agreement in the full range of q can be obtained by using the slightly modified expression $\langle \omega_q \rangle \propto \sqrt{1+p^2 \sin^2(qd)}$, in which p is now an adjustable parameter. The best fit of this relation to the experimental data is achieved with a value $p \approx 3.1$ (bold-dot-dashed line in Fig. 10). The fact that p differs again by a factor 2.5 from its SMA value implies the existence of a *non-negligible* spectral weight above the gap, which leads to an increase of $\langle \omega_q \rangle$ and to a decrease of $S(q)$. We believe that the extra intensity in $CuGeO_3$ observed well above the gap originates from the continuum of magnetic excitations predicted to exist in the ideal alternating antiferromagnetic chain,[9] as well as in the uniform antiferromagnetic chain. For this model, theory predicts[4] a slowly decaying structure factor

$$S(q_c,\omega) \propto [\omega^2 - \omega_1^2(q_c)]^{-\alpha} \Theta(\omega - \omega_2(q_c)),$$

where $\Theta(x)$ is the ''step'' function and $\alpha \approx 0.5$–0.6. The window is limited on the low-energy side by $\omega_1(q_c)$ (defined previously) and on the high-energy side by $\omega_2(q_c) \approx 2\pi J \sin(q_c d/2)$, with $2\pi J \approx 30$ meV in the case of $CuGeO_3$. However, such a behavior is not observed in $CuGeO_3$. Our experimental results on $S(q_c,\omega)$ and $S(q_c)$ can be understood if we assume that the dynamic structure factor is composed of two different parts: a narrow peak centered at the gap energy, followed by a broad contribution of much smaller amplitude, but extending well above the gap and carrying a roughly equivalent spectral weight. As discussed previously, the high-energy contribution might be associated with some sort of continuum.

Recent numerical calculations performed by exact diagonalization[13] of finite-size alternating systems have allowed a quantitative understanding of the wave-vector dependencies of the equal-time structure factor. The bold-dashed line in Fig. 10 represents the theoretical $S(q)$ calculated numerically by Grempel *et al.*,[13] starting from the Hamiltonian (1) with an alternation parameter $\alpha \approx 0.9$, which corresponds approximately to the experimental determination. As can be seen, the experimental data are quite well reproduced by the calculations, in the full range of q values. Unfortunately, calculation of $S(q,\omega)$ for the ideal alternating chain at small $1-\alpha$ seems unable to reproduce the experimental line shape, the theoretical prediction being not very different from that of the uniform chain. At least, interchain couplings should be taken into account in improved calculations.

As proposed in Ref. 13, the breakdown of the SMA (originating from the continuum) should explain the factor 2 in the relationship of Δ to $1/\xi$. Accordingly, the product $\Delta.\xi$ appears to have no universal character. This is well illustrated by considering the exactly solvable spin-1 Heisenberg model with a biquadratic exchange,[65,66] described by the Hamiltonian $H = J\Sigma_i[\mathbf{S}_i\mathbf{S}_{i+1} + \frac{1}{3}(\mathbf{S}_i\mathbf{S}_{i+1})^2]$. For this model one knows that $\Delta \approx 0.75J$, $\xi/d \approx 1/\ln 3 \approx 0.91$, whereas

$$S(q) \propto \frac{1-\cos(2\pi q d)}{5/3+\cos(2\pi q d)}.$$

It is easy to verify that Δ and ξ are related by $\Delta\xi \approx 0.68Jd$, which is now a factor 3.5 smaller than the spin-wave velocity $c_0 \approx 2.7Jd$. Clearly, there is no universal relation between Δ and ξ, whereas $S(q)$ for that model does not agree with the SMA expression, especially not in the vicinity of $q=0$. This is precisely the signature of the continuum, which for $S=1$ occurs at $q=0$ and not at $q=\pi$ as for $S=1/2$.

D. Temperature dependence of the magnetic excitations

X-ray measurements by Pouget *et al.*[45] have unambiguously revealed the existence of relatively strong anisotropic structural fluctuations, visible at least up to 40 K. Due to magnetoelastic couplings, the correlation length associated with these fluctuations is typically of the same order of magnitude as the magnetic dynamic correlation length for temperatures in the range T_{SP}–25 K. One might therefore assume that the magnetic system will not recover completely the properties of an ideal spin-1/2 HAF system, in the case of important spin-lattice couplings. More precisely, the existence in $CuGeO_3$ of quasi-1D structural correlations has been thought to induce the formation of a pseudogap[45] in the excitation spectrum above T_{SP}. Such a feature, whenever it exists, could explain the quite unusual behavior of the magnetic susceptibility observed above the SP transition temperature,[33] which deviates strongly from the Bonner-Fisher prediction established for the ideal spin-1/2 HAF chain. Previous INS measurements by Nishi, Fujita, and Akimitsu[35] at $\mathbf{q}=\mathbf{k}_{\mathrm{AF}}$ and Regnault *et al.*[36] at $\mathbf{q} \neq \mathbf{k}_{\mathrm{AF}}$ have come to contradictory conclusions concerning the possible existence of a pseudogap above T_{SP}. In order to more carefully investigate its existence, we have performed accurate

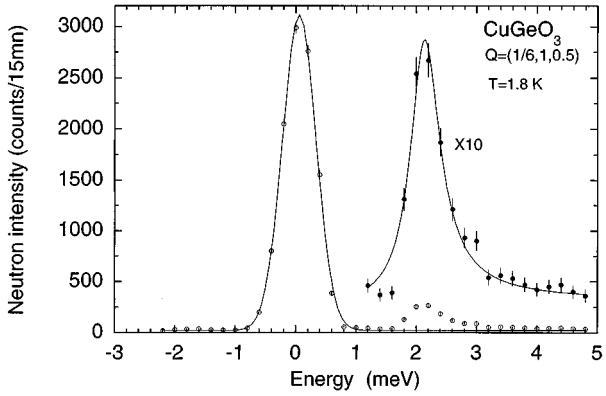

FIG. 11. Constant-Q scans at $\mathbf{Q}=(1/6,1,1/2)$ and $T=1.8$ K showing the relative intensities of the incoherent scattering (around $\omega=0$) and the inelastic scattering (around $\omega=2$ meV). The solid lines are fits to Gaussian and Loretzian functions, respectively.

INS experiments on the DN1 thermal neutron spectrometer, at various temperatures below and above T_{SP}, and for several values of the wave vector.

We have performed energy scans at a fixed scattering vector $\mathbf{Q}=(1/6,1,1/2)$, slightly shifted along the a^* axis from the antiferromagnetic point $\mathbf{k}_{AF}$. The main reason for this choice arises from the necessity to control the accuracy of the temperature by measuring directly and simultaneously the temperature dependence of the superlattice peak (1/2,3,1/2). The elastic-incoherent contribution and the background contribution have been determined from an energy scan recorded at the lowest temperature. This scan is shown in Fig. 11. The resulting contribution has been analyzed, following the standard procedure, from a Gaussian function of energy:

$$I(\omega)\approx I_{BG}+I_0\ \exp\left[-4\ln 2\left(\frac{\omega-\delta\omega}{\Delta\omega}\right)^2\right]. \qquad (11)$$

In this expression, the FWHM $\Delta\omega$ represents the instrumental resolution in energy, whereas $\delta\omega$ is an offset in energy originating from a slight misalignment of the analyzer crystal. The best fit is achieved with parameters $I_{BG}\approx 30$, $I_0\approx 3120$, $\Delta\omega\approx 0.64$ meV, and $\delta\omega\approx 0.07$ meV. This contribution has been systematically subtracted from the various energy scans, in order to obtain the purely magnetic part of the signal. Figure 12(a) shows typical corrected experimental data obtained at temperatures $T=1.8$, 13.5 ($T<T_{SP}$), and 15.15 K ($T>T_{SP}$). At $T=1.8$ K, the maximum intensity is observed at 2.1 meV, a value only *slightly* larger than the gap value. This means that the fact of having performed measurements at $q_a=1/6$ instead of $q_a=0$ should not affect dramatically the conclusions. The resulting magnetic response is strongly modified when crossing T_{SP}, evolving from a purely inelastic regime at low temperature toward an overdamped regime above T_{SP}. Both a damping and a renormalization of the gap mode are observed when T_{SP} is approached from below. In absence of more accurate theoretical calculations, the experimental data at finite temperature have been analyzed using the following scattering function:

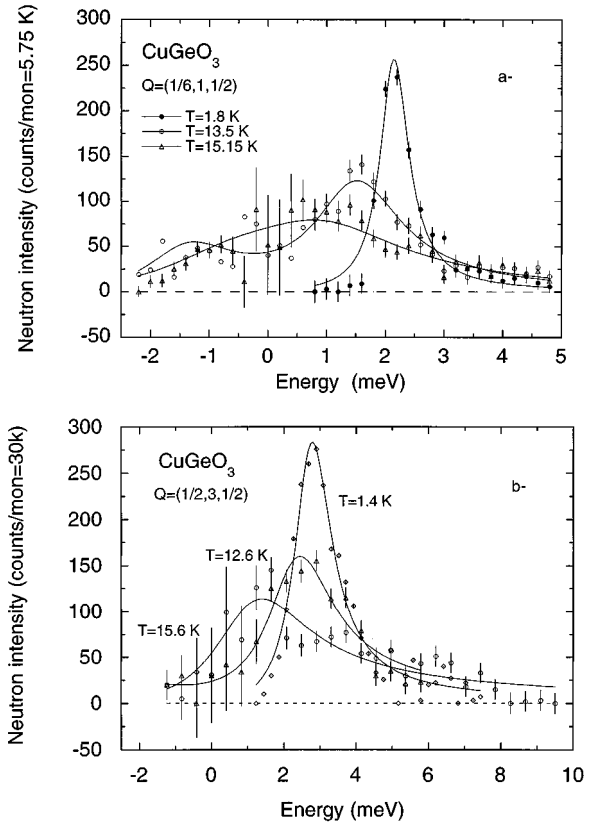

FIG. 12. (a) Constant-Q scans at $\mathbf{Q}=(1/6,1,1/2)$ for various temperatures located below (1.8 and 13.5 K) and above (15.15 K) T_{SP}; (b): Constant-Q scans at $\mathbf{Q}=(1/2,3,1/2)$ for various temperatures located below (1.4 and 12.6 K) and above (15.6 K) T_{SP}. In both cases, the solid lines are fitted using relation (12), according to the procedure described in the text.

$$S(k_{AF},\omega)\approx\frac{S_0}{\Gamma}\frac{\omega}{1-\exp\left(-\frac{\omega}{kT}\right)}\left[\frac{1}{1+\left(\frac{\omega-\Delta}{\Gamma}\right)^2}+\frac{1}{1+\left(\frac{\omega+\Delta}{\Gamma}\right)^2}\right], \qquad (12)$$

where S_0 is a normalization factor and Γ the damping parameter. Although lacking precise theoretical justification, such an expression has the practical advantage of displaying a continuous change from an inelastic behavior when $\Delta/\Gamma\gg 1$ to a quasielastic behavior when $\Delta/T\ll 1$. We have found that Eq. (12) reproduces better the experimental data in the vicinity of the transition temperature than a damped-harmonic-oscillator function. In the fitting procedure, the function given by Eq. (12) has been convoluted with the instrumental resolution function in energy, $R(\omega)$, according to the relation $I(\omega)\propto k_f^3\cot g(\theta_a)S(\omega)*R(\omega)$, where the neutron quantities k_f and θ_a have their usual meaning.[67] The best fit of experimental data to the above relation results in the set of parameters Δ and Γ versus T listed in Table III, using a Gaussian resolution function of FWHM 0.7 meV. The resulting dependencies for $\Delta(T)$ and $\Gamma(T)$ are depicted in Fig. 13. In agreement with previous INS results,[35] the gap value starts to decrease only above 11 K, whereas the damping increases

TABLE III. Temperature dependence of the gap energy (Δ) and damping (Γ) at $\mathbf{Q}=(1/6,1,1/2)$.

T (K)	Δ (meV)	Γ (meV)
1.8	2.10	0
9.2	2.05	0.20
10.96	1.99	0.35
12.33	1.84	0.55
12.80	1.74	0.55
13.50	1.45	0.75
14.05	0.90	1.25
15.15	0.50	1.50
19.60	0.0	2.20

rapidly in the vicinity of T_{SP}. Not very surprising, the experimental form of $\Delta(T)$ cannot be reproduced by a conventional BCS relation, the experimental results showing a more ''steplike'' behavior in the vicinity of T_{SP}. If we assume the gap to be mainly induced by the dimerization, this non-BCS behavior should qualitatively find its origin in the existence of lattice correlations observed above the SP transition temperature. However, a more quantitative analysis of these data would require going beyond the mean-field approach. Unfortunately, such a theory is not yet available. Nevertheless, our experimental results show that the spin gap $\Delta(T)$ takes a *finite* value at T_{SP}, verifying the relation $\Delta(T_{SP})\approx\Delta(0)/2$, whereas one has simultaneously $\langle\delta\rangle_{T_{SP}}\approx 0$, as seen directly from the temperature dependence of the superlattice peak (1/2,3,1/2).

Due to the overdamped character of the magnetic response above T_{SP}, it is more difficult to get accurate values of Δ, than to determine Γ. For example, at $T=15.15$ K, the best fit is achieved with a finite value $\Delta\approx 0.5$ meV. However, varying Δ between 0 and 1 meV hardly changes the quality of the fit. At 20 K, the best fit is achieved with a value $\Delta\approx 0$, which suggests a rapid vanishing of the pseudogap as T increases. In fact, the important damping which takes place above T_{SP} has strongly limited any precise determination of the gap value above typically 16 K. Our experimental results for the particular component $q_a=1/6$ are consistent with a picture, following which the pseudogap exists only in a limited range of temperatures above T_{SP}. In fact, it is observed only when the various structural correlation lengths have reached sufficiently large values. According to the x-ray critical scattering measurements of Pouget *et al.*,[45] an intrachain structural correlation length $\xi_c^{\text{struc}}\approx 17c\approx 4-5\xi_c^{\text{mag}}\approx 50$ Å is observed at 15 K, whereas the pseudogap energy appears strongly reduced and damped at the same temperature. Quite consistently, Renard *et al.*[69] have shown that the substitution of only $x\approx 1\%$ of Ge by Si atoms (which corresponds to an average Si-Si distance of $c/x\approx 100c$ in 1D and $c/\sqrt[3]{x}\approx 5$ in 3D) is strong enough to destroy the SP ground state and the spin gap, inducing below a Néel temperature $T_N\approx 4.5$ K a 3D magnetic long-range ordering described by the propagation vector $\mathbf{k}_{AF}$. Actually, the magnetic gap at $\mathbf{q}=\mathbf{k}_{AF}$ requires, to develop, that a relatively *large* number of dimers exist in the correlated segments. More quantitatively, the pseudogap is present when roughly $\xi_c^{\text{struc}}>5-10c$, which also implies a large number of correlated atoms in both directions perpendicular to the chain axis. Consequently, the spin gap appears as a typically 3D feature.

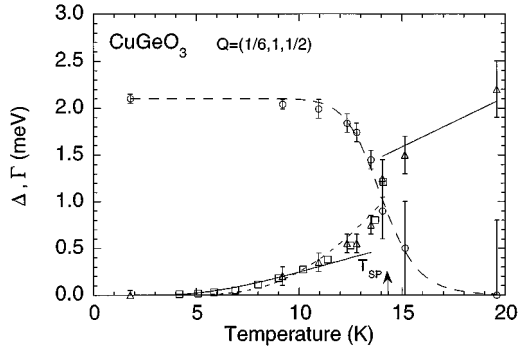

FIG. 13. Temperature dependencies of the gap energy ($\triangle$) and the damping parameter (Γ). Open circles and triangles are the experimental points obtained by INS. The open squares correspond to rescaled NMR data taken from Ref. 39. The various lines correspond to calculated or fitted curves as described in the text.

TABLE IV. Temperature dependence of the gap energy (Δ) and damping (Γ) at $\mathbf{Q}=(1/2,3,1/2)$.

T (K)	Δ (meV)	Γ (meV)
1.40	2.7	0
12.60	2.2	0.5
15.6	1.1	1.2

A more pronounced inelastic character is observed when the difference $|\vec{q}-\vec{k}_{AF}|$ increases, as shown by measurements of the temperature dependence of the spin dynamics around $\mathbf{k}_{SP}$ (i.e., for $q_a=1/2$). Although less exhaustively, some measurements were performed on the 1T thermal-neutron spectrometer at a scattering vector $\mathbf{Q}=(1/2,3,1/2)$. Following the same analysis procedure, we were able to extract the purely magnetic contribution from both sides of T_{SP}. Figure 12(b) shows the resulting data for three typical temperatures $T=1.4$, 12.6, and 15.6 K located below and above T_{SP}. In contrast to the previous case, the magnetic response at 15.6 K appears clearly *inelastic*, displaying a well-defined maximum at about 1.6 meV. The data were analyzed quantitatively from Eq. (12), with the parameters Δ and Γ listed in Table IV. The value obtained for Δ at 15.6 K confirms quantitatively the behavior qualitatively described above: the response is inelastic at $q_a=1/2$, with a characteristic energy scale that reflects the dispersion resulting from the interchain couplings J_a', $(\Delta E)_a\approx 1.6$ meV. The same remark can be made at $q_a=1/6$, where we have obtained an inelasticity compatible with the relation $(\Delta E)_a\sin(\pi/6)\approx 0.8$ meV. This fact can be understood if damped and renormalized magnetic excitations persist above T_{SP} for sufficiently large values of $|\vec{q}-\vec{k}_{AF}|$, a feature typical of low-dimensional magnetic systems.[70–72] As expected for such systems, the renormalization depends strongly on the ratio $\omega(q_a)/T$, and should be less important at large values than at small values. We believe that the inelasticity observed well above T_{SP} at large q_a (or q_b, where the effect should be stronger) can be understood as an effect of the dispersion originating from interchain couplings. Extrapolating the results obtained at $q_a=1/2$

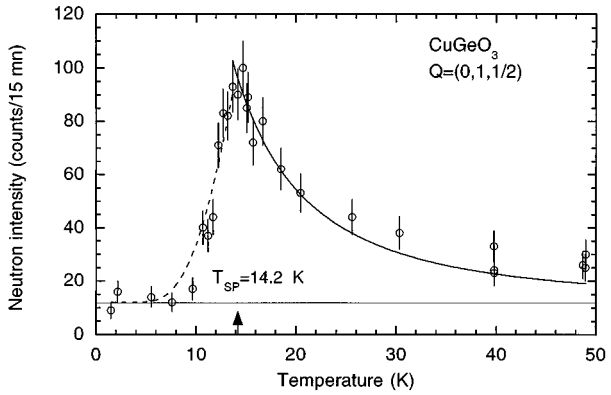

FIG. 14. Temperature dependence of the magnetic intensity at the scattering vector $\mathbf{Q}=(0,1,1/2)$ and energy $\omega=1$ meV. Open symbols are the experimental points. The solid line is a fit to a $1/T^2$ law. The dashed line is a fit to an activation law, with an activation energy $2\Delta\approx4$ meV.

and 1/6 to $q_a=0$, we are again lead to assume that the spin-gap in the excitation spectrum must be *small* in the temperature range 15.2–15.6 K. On the other hand, our measurements give strong support for a *finite* value of the gap at T_{SP}.

The point of view of a rapidly vanishing gap above T_{SP} has been further confirmed by studying the temperature dependence of the inelastic scattering at position $\mathbf{Q}=(0,1,1/2)$ and for an energy transfer $\omega\approx1$ meV located in the gap. Figure 14 shows the results obtained using the DN1 spectrometer. Experimentally, one observes a maximum of scattering roughly at T_{SP}, with an intensity above the transition temperature relatively well described by a $1/T^2$ law typical of a *gapless* quasi-1D system.[70] Once again, this strongly suggests a relatively rapid disappearance of the pseudogap above the SP-transition temperature.

A further test of theoretical predictions is obtained from a plot of the gap value $\Delta(T)$ versus $\sqrt{I_D(T)}$ for $T<T_{SP}$, $I_D(T)$ being the intensity of a superlattice peak measured at temperature T. This quantity is simply related to the order parameter $\langle\delta\rangle_T$ (previously defined) by the relation $I_D(T)\propto(\langle\delta\rangle_T)^2$. Such a procedure may allow us, among other things, to determine experimentally the relationship of $\Delta(T)$ to $\langle\delta\rangle_T$, assuming negligible changes in J with T. Figure 15 shows the experimental data which were obtained.

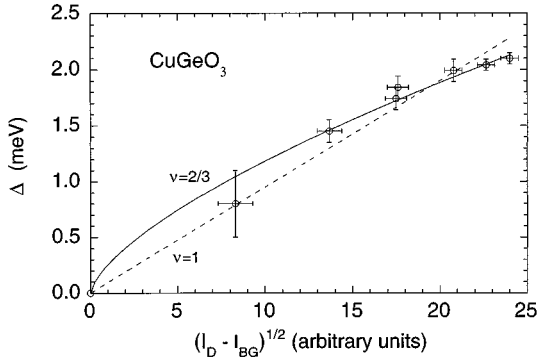

FIG. 15. Plot of the gap energy Δ as a function of the square root of the intensity at the point (1/2,3,1/2). The solid and dashed lines are fits to power laws, as described in the text.

From the theoretical side, power-law relations of type $\Delta(T)\propto(\langle\delta\rangle_T)^\nu$ have been predicted, with values of ν ranging from 2/3 to 1, depending on the model or approach used (see Sec. I). In Fig. 15 the solid line is calculated with $\nu=2/3$, whereas the dashed line is calculated with $\nu=1$. Taking into account the experimental accuracy, the former value seems to better describe the present neutron data, giving additional support to the approach of Cross and Fisher.[7] Recent numerical calculations on the alternating chain[13] have given a slightly larger value $\nu=0.69\pm0.01$, which also agrees with the experimental determination.

The temperature dependence of the damping parameter Γ is shown in Fig. 13, for values of the temperature on both sides of T_{SP}. In this figure we also show rescaled values of $1/T_1T$ obtained from NQR measurements,[39] a quantity which should reflect closely the behavior of $\Gamma(T)$. This statement can be derived from Eq. (12), starting from the well-known NMR relation between $1/T_1$ and $S(q,\omega)$:

$$1/T_1\propto\sum_q (A_q)^2 S(q,\omega\approx0)\propto\sum_q (A_q)^2 \lim_{\omega\to0}\frac{\chi''(q,\omega)}{\omega}$$

[A_q being the Fourier transform of the hyperfine coupling constants and $\chi''(q,\omega)$ the imaginary part of the generalized susceptibility]. Assuming an inelastic Lorentzian form for the response function $\chi(q,\omega)$ [from which relation (12) results], one can easily obtain the relation $1/T_1T\propto\Gamma(T)/\Delta^2$, which is in good agreement with the neutron data below T_{SP} (see Fig. 13). Two different behaviors are observed, depending on whether T is smaller or larger than T_{SP}. At low temperature ($T<10$ K), Γ increases rapidly with T, following approximately an exponential dependence. The solid line in Fig. 13 is a fit to the simple relation $\Gamma(T)\approx\Gamma_0\exp(-\Delta/kT)$ with parameters $\Delta\approx24$ K and $\Gamma_0\approx2.7$ K, whereas the dashed line is a fit to the relation $\Gamma(T)\approx\Gamma_0\exp(-2\Delta/kT)$ with $\Delta\approx24$ K and $\Gamma_0\approx30$ K. Without an explanation so far, the latter expression seems to reproduce better the experimental data in a larger temperature range. However, in the absence of a more accurate theory, it is difficult to say more on the physical meaning of these parameters. Finally, the data below T_{SP} shown in Fig. 14 can be roughly reproduced by the relation $S(T)\approx2700\exp(-2\Delta/kT)$ with $\Delta\approx24$ K, which can be qualitatively understood from the relation $S(T)\propto\Gamma(T)/\Delta^2$, assuming again for $\Gamma(T)$ an activation law with an activation energy 2Δ and a magnetic correlation length almost independent of T.

Above T_{SP}, Γ recovers a much weaker temperature dependence, following approximately the linear relation $\Gamma\approx kT$. Such a behavior is expected for the ideal Heisenberg chain.[70] However, it is difficult to make any definitive conclusions, owing to the small temperature range explored in the present experiment. Recent specific-heat measurements[42] carried out on a single crystal have given some evidence for a quasi-2D behavior above T_{SP}, recognized from the existence of a T^2 term in the magnetic specific heat. Obviously, this behavior is in disagreement with the neutron-scattering determination of $S(T)$ previously described, which has revealed a rather strong 1D character.

Integrating over the inelastic peak has allowed us to get information on the temperature dependence of the structure factor at the antiferromagnetic point $S(\mathbf{k}_{AF},T)$. In the sim-

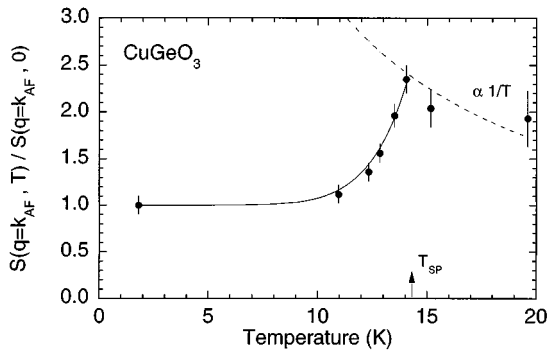

FIG. 16. Temperature dependence of the reduced energy-integrated intensity at the antiferromagnetic point $S(k_{\mathrm{AF}},\omega)/S(k_{\mathrm{AF}},0)$. The solid line corresponds to $1/\Delta(T)$. The dashed line is a fit to the classical prediction for a quasiuniform antiferromagnetic chain.

plest 1D model, this quantity should reflect directly the behavior of the intrachain magnetic correlation length ξ, since we should have $S(\mathbf{k}_{\mathrm{AF}}, T)\propto\xi(T)$ after Eq. (10). Figure 16 shows the experimental results for the normalized ratio $S(\mathbf{k}_{\mathrm{AF}}, T)/S(\mathbf{k}_{\mathrm{AF}}, 0)$ obtained from the inelastic scans versus temperature previously described. $S(\mathbf{k}_{\mathrm{AF}}, T)$ is found to first increase with increasing temperature, go through a maximum near T_{SP} and then decrease again at higher temperatures. Above T_{SP}, the experimental data can be accounted for by the relation $\xi(T)\propto 1/T$, which again is characteristic of quasi-1D fluctuations. The dashed line in Fig. 16 is calculated from the more quantitative relation $\xi(T)/\xi(0)\approx 34/T$ (with T expressed in Kelvin). By introducing the value of the correlation length at $T\approx 0$ previously determined [namely $\xi(0)\approx 3c$], one gets $\xi(T)/c\approx 102/T$, a relation which is in quantitative agreement with the theoretical prediction for the spin-1/2 HAF chain $\xi(T)/c\approx 2JS(S+1)/kT\approx 90/T$, taking for J the average value $J\approx J_1[(1+\alpha)/2]\approx 5.1$ meV. In our opinion, the good quantitative agreement between experimental and theoretical prefactors confirms the quasi-1D nature of the magnetic fluctuations above T_{SP} in $CuGeO_3$.

Unfortunately, below T_{SP} at finite temperature, there is no *precise* theory capable of reproducing the present experimental data. However, in this range of temperatures, $S(\mathbf{k}_{\mathrm{AF}}, T)$ seems to reflect closely the behavior of $1/\Delta(T)$. The solid line in Fig. 16 is calculated from the simple relation $S(\mathbf{k}_{\mathrm{AF}}, T)/S(\mathbf{k}_{\mathrm{AF}}, 0)\approx 2.0/\Delta(T)$, using for $\Delta(T)$ the experimental determination. Such a relation is expected in the single-mode approximation, which is believed to be crude at $\mathbf{q}=\mathbf{k}_{\mathrm{AF}}$ for the ideal 1D system (see Sec. III C). If the relation between $S(\mathbf{k}_{\mathrm{AF}})$ and ξ remains valid at finite temperature, then the product $\xi(T)\Delta(T)$ appears as more or less constant in the SP phase. The value of this constant amounts to about 18 ± 3 meV Å, that is to say about half the experimental spin-wave velocity $c_0\approx 39$ meV Å. As already pointed out, Δ and ξ follow closely the empirical relation $2\Delta\approx c_0/\xi$, even at finite temperature. This may be an indication that the continuum (responsible for the factor 2 above) is weakly temperature dependent, at least up to T_{SP}.

IV. NEUTRON SCATTERING UNDER FIELD

The application of a magnetic field is expected to have dramatic effects on the spin system, and should also induce, through the spin-lattice couplings, significant modifications of the lattice properties. Consequently, both the spin dynamics and the lattice distortion should be sensitive to the application of a magnetic field. In particular, one expects the nonmagnetic singlet ground state to be destroyed above a characteristic critical field $H_c\approx 0.84\Delta/g\mu_B$ (see Sec. I), the SP system recovering in this part of the H-T phase diagram a more or less well-defined magnetic ground state. Magnetization measurements on powdered samples[34] and a single crystal[41] of $CuGeO_3$ have clearly demonstrated the existence of such a critical field at $H_c\approx 125$ kOe$\approx 0.83\Delta/g\mu_B$, in good agreement with the mean-field predictions of Bray[16] and Cross.[15] Above H_c, the magnetization is expected to vary as $(H-H_c)^{1/2}$, following the same prediction as for the alternating chain.[20]

In case of weak spin-lattice couplings, the triplet excited state should split into three distinct components Δ_-, Δ_0, and Δ_+, displaying quasilinear dependencies at small H, according to the simple relations:

$$\Delta_-(H)\approx\Delta-g\mu_B H, \tag{13a}$$

$$\Delta_0(H)\approx\Delta, \tag{13b}$$

$$\Delta_+(H)\approx\Delta+g\mu_B H. \tag{13c}$$

Such relations can be derived from a simple perturbational treatment of the Zeeman term.[19,73] Equation (13a) predicts a critical field of $H_c\approx\Delta/g\mu_B$. Obviously, nonlinear effects should take place near H_c, in particular to account for the fact that $g\mu_B H_c$ is about 16% smaller than Δ. According to the SP theory, the transition temperature T_{SP} is predicted to decrease slightly as the field increases, following a quadratic dependence on field at low field given by the relation:

$$T_{\mathrm{SP}}(H)\approx T_{\mathrm{SP}}(0)\left[1-t\left(\frac{g\mu_B H}{2kT_{\mathrm{SP}}(0)}\right)^2\right] \tag{14}$$

with a coefficient t ranging from 0.365 (Ref. 14) to 0.44 (Ref. 15). High-field magnetization measurements on *polycrystalline* samples[34] have allowed a precise verification of Eq. (14) in $CuGeO_3$, with a coefficient $t\approx 0.4$ between the two theoretical determinations. Unfortunately, if the magnetization above H_c has been carefully studied and seems to be well understood, little is known regarding the field dependence of the main characteristics associated with the lattice distorsion itself. From theoretical arguments, the wave vectors associated with the 3D lattice distortion ($\mathbf{k}_{\mathrm{SP}}$) and the magnetic 1D staggered short-range correlations ($\mathbf{k}_{\mathrm{AF}}$) are expected to remain unchanged up to H_c, but should become *incommensurate* above this field value, the shift to commensurability increasing with H more or less proportionally to the magnetization.[15,74] The incommensurate character of the lattice distortion has been recently observed in TTF-CuBDT from x-ray measurements.[32] However, nothing has been reported so far concerning the magnetic counterpart. In $CuGeO_3$, the existence of sizable interchain couplings could very likely induce a more or less incommensurate 3D magnetic *long-range* ordering (soliton lattice), which should be detectable by neutron diffraction.

In order to clarify the situation, we have undertaken neutron-scattering measurements under a magnetic field ap-

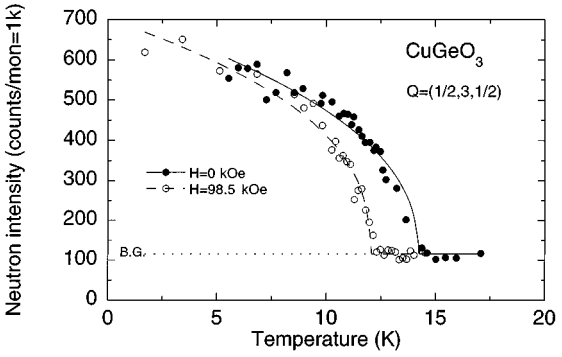

FIG. 17. Temperature dependence of maximum intensity of superlattice peak (1/2,3,1/2) for two values of the magnetic field $H=0$ and $H=98.5$ kOe. The various lines are fits to power laws, as described in the text.

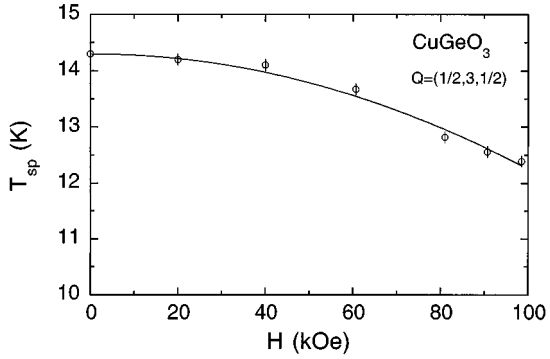

FIG. 18. Field dependence of the spin-Peierls transition temperature determined from the superlattice peak (1/2,3,1/2). The solid line is a fit to the theoretical prediction, as explained in the text.

plied perpendicular to the chain axis, for field values up to 10 T. These experiments were performed on the DN1 thermal three-axis spectrometer, using experimental conditions described in Sec. II. We will discuss successively the effects of an applied magnetic field on the SP transition temperature $T_{SP}(H)$, the lattice distortion $\delta(H)$ and the various dynamic structure factors $S_\nu(q,\omega)$,($\nu=x$, y, and z).

A. Field dependences of T_{SP} and δ

The SP-transition temperature under field was obtained by recording the temperature dependence of the neutron intensity at position $\mathbf{Q}=(1/2,3,1/2)$. Figure 17 shows the evolution with temperature of the intensity for the two extreme values of the magnetic field, $H=0$ and $H=98.5$ kOe. $T_{SP}(H)$ was determined following a similar analysis procedure, as previously described in Sec. III A. In agreement with high-field magnetization measurements,[34] $T_{SP}(H)$ displays a slight decrease of the order of 13% between 0 and maximum field. The values obtained for $T_{SP}(H)$ are listed in Table V. The corresponding experimental data are displayed in Fig. 18 as a function of field. They were successfully fitted to the theoretical expression (13). The best fit is achieved with a prefactor $t\approx 0.52\pm 0.05$, significantly larger than the theoretical prediction $t\sim 0.4$. Our determination of the coefficient t seems to lead to values slightly larger than other experimental determinations obtained from magnetization[34] and x-ray diffraction[53] measurements. However, the experimental consensus seems to indicate for t a value slightly larger than the mean-field theoretical predictions. Again, we have attributed the faster experimental decrease of $T_{SP}(H)$ to an effect of structural fluctuations, which were completely neglected in the various theoretical approaches.

TABLE V. Field dependence of the spin-Peierls transition temperature T_{SP} and the gaps Δ_-, Δ_0, and Δ_+ at $\mathbf{Q}=(1/6,1,1/2)$.

H (kOe)	T_{SP} (K)	Δ_- (meV)	Δ_0 (meV)	Δ_+ (meV)
0	14.30	2.0	2.0	2.0
20	14.20	1.8	2.0	2.2
40	14.10	1.55	2.0	2.45
60.7	13.67	1.20	2.0	2.80
80.7	12.82	1.02	2.0	3.02
90.7	12.56			
98.5	12.39	0.70	2.0	3.3

In a quite similar manner as for $H=0$, we have obtained at maximum field a value of the exponent $\beta\approx 0.28\pm 0.03$ which is nearly identical to the previous one in zero field, taking into account the experimental accuracy. Figure 1 shows a comparison between two longitudinal Q scans performed across the superlattice peak (1/2,3,1/2) at field values $H=0$ and $H=81$ kOe. The background intensity, mainly arising from the fourth-order-nuclear-Bragg contamination (not filtered in our experiment), was determined at 25 K, a temperature which is sufficiently far from T_{SP}. Quite surprisingly, *no change* in peak intensity, in peak width, or in peak position could be detected in these measurements, at least up to 100 kOe (i.e., below $0.77H_c$). This was further confirmed with more accuracy by measuring the integrated intensities of several superlattice peaks at about 98 kOe (in fact the same peaks as in zero field). We have performed ω scans across these peaks at two different temperatures, 5 and 23 K, located below and above T_{SP}, respectively. The contribution associated with the lattice distortion was deduced by substracting the data obtained at the highest temperature from the data obtained at low temperature. Spurious effects sometimes encountered in high magnetic field (like, e.g., unexpected sample displacements or mechanical effects due to the strong stray fields) were controlled by measuring systematically the nuclear Bragg peaks (0 0 1), (1 4 0), and (1 6 0). The integrated intensities which were obtained, corrected by the Lorentz factor, are listed in Table I for the four typical superlattice peaks previously considered. Clearly, no change in intensity is observed within the experimental error bars, implying very weak changes in displacements of both Cu and O(2) atoms under field, at least up to 100 kOe. The situation is very different from that existing in TTF-CuBDT, for which a reduction in intensity of about 35% was observed by neutron[31] and x-ray[32] diffraction. This steeper decrease may be directly correlated to the larger value of β observed in TTF-CuBDT ($\beta\approx 0.5$ instead of $\beta\approx 0.26$ in $CuGeO_3$), reflecting the higher dimensionality of the structural fluctuations in the former compound.

B. Field dependence of the spin dynamics

In order to test directly the correlation between the spin-gap and the lattice distortion, we have determined the field

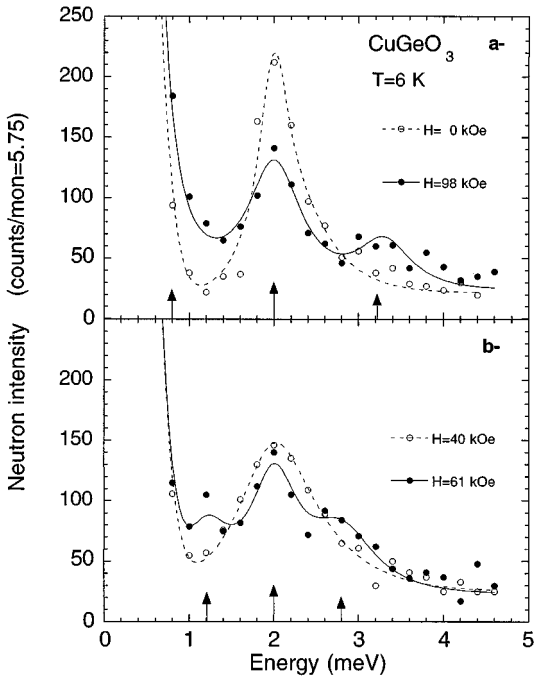

FIG. 19. Constant-Q scans at $\mathbf{Q}=(1/6,1,1/2)$ and $T=6$ K, for different values of the magnetic field. (a) $H=0$ and $H=98$ kOe; (b): $H=40$ and $H=61$ kOe. The lines are fits as explained in the text.

dependence of the spin dynamics in the vicinity of the antiferromagnetic point $\mathbf{k}_{\mathrm{AF}}$. For this purpose, energy scans were performed at a temperature of 6 K (located sufficiently well below T_{SP}) and at a scattering vector $\mathbf{Q}=(1/6,1,1/2)$, slightly shifted from $\mathbf{k}_{\mathrm{AF}}$ along the a^* direction (i.e., the direction for which the 1D character is the best). Figures 19(a) and 19(b) show typical results obtained at fields $H=0$ and 98 kOe, and $H=40$ and 61 kOe, respectively. A splitting of the magnetic mode is unambiguously observed in increasing field and three gap modes exist at high field, confirming the triplet ($S=1$) nature of the first excited state. These results are consistent with previous INS experiments in lower field values.[75] The lowest and highest gap modes are found to, respectively, decrease and increase with increasing field, whereas the third mode remains constant within the experimental errors. The experimental data were analyzed by assuming (for simplicity) Gaussian profiles for all modes. The solid and dashed lines in Figs. 19 correspond to the best fit of experimental data to a response function which is the sum of three such Gaussian functions. The values which were obtained for the gaps Δ_-, Δ_0, and Δ_+ are listed in Table VI. Figure 20 shows the resulting field dependencies of the gap values for fields up to almost 100 kOe. As expected, quasilinear dependencies are observed, for all modes. By fitting the experimental results to Eq. (12), we obtained $\Delta\approx 2$ meV and $g_x\approx 2.18$, which are in quantitative agreement with the previous neutron data at lower field reported by Fujita *et al.*[75] From the energy scans shown in Figs. 19(a) and 19(b), one can estimate the energy-integrated intensity of each of the three gap modes. Table VI summarizes the field dependence of the partial intensities I_-, I_0, I_+ and the total intensity $\Sigma I=I_-+I_0+I_+$, after correction by the neutron normalization factor $k_f^3\cot g(\theta_a)$. Within the experimental errors, we have obtained that the total intensity ΣI is maintained between 0 and 100 kOe (with a value $\Sigma I=148\pm 15$), whereas one has approximately the relation $I_+\approx I_-\approx I_0/2$ (within an accuracy of the order of 10%), for any field. In fact, these results are reminiscent of those obtained for the field dependence of the gap-mode intensities in the $S=1$ Haldane gap system NENP (see Ref. 76). Unfortunately, there is no precise theory giving the field dependence of the various structure factors, neither for the SP system nor for the alternating chain.[20] Quite generally,[77] the intensities of various modes at a scattering vector $\mathbf{Q}=(0,Q_y,Q_z)$ can be written as (x being the direction of the applied field):

$$I_-\approx S_-^x+\left[1-\left(\frac{Q_y}{Q}\right)^2\right]S_-^y+\left[1-\left(\frac{Q_z}{Q}\right)^2\right]S_-^z, \quad (15a)$$

$$I_0\approx S_0^x+\left[1-\left(\frac{Q_y}{Q}\right)^2\right]S_0^y+\left[1-\left(\frac{Q_z}{Q}\right)^2\right]S_0^z, \quad (15b)$$

$$I_+\approx S_+^x+\left[1-\left(\frac{Q_y}{Q}\right)^2\right]S_+^y+\left[1-\left(\frac{Q_z}{Q}\right)^2\right]S_+^z. \quad (15c)$$

Now, if we assume that mode (0) is mainly x polarized (implying $S_0^y\approx S_0^z\approx 0$), and that mode $(-)$ and mode $(+)$ are mainly isotropically yz polarized (implying $S_-^x\approx S_+^x\approx 0$) as is expected from general arguments,[78] the above expressions can be rewritten as

$$I_-\approx\left[1-\left(\frac{Q_y}{Q}\right)^2\right]S_-^y+\left[1-\left(\frac{Q_z}{Q}\right)^2\right]S_-^z, \quad (16a)$$

TABLE VI. Field dependence of the partial intensities (I_-, I_0, and I_+) and total intensity ($\Sigma I=I_-+I_0+I_+$) associated with the various gap modes.

H (kOe)	I_-	I_0	I_+	ΣI
0	36	72	36	143±15
20	34	66	34	134±15
40	37±4	76±7	37±4	150±15
60.7	39±4	78±7	48±4	165±15
80.7	38±4	69±7	34±4	141±15
98.5	45±4	77±7	34±4	156±15

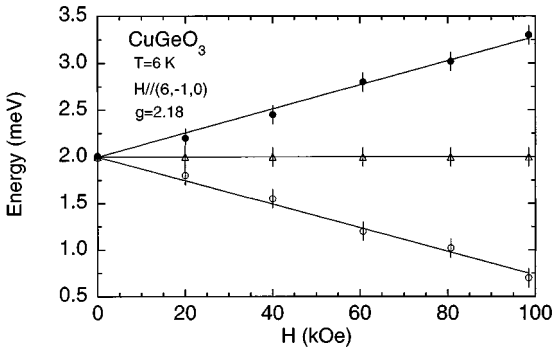

FIG. 20. Field dependence of the gap energies at "$q=\pi$" and temperature $T=6$ K, in a field applied perpendicular to the chain axis. The solid lines correspond to the theoretical prediction given by Eqs. (12).

$$I_0 \approx S_0^x, \tag{16b}$$

$$I_+ \approx \left[1-\left(\frac{Q_y}{Q}\right)^2\right] S_+^y + \left[1-\left(\frac{Q_z}{Q}\right)^2\right] S_+^z . \tag{16c}$$

The total intensity is calculated from the following relation:

$$\Sigma I \approx S_0^x + \left[1-\left(\frac{Q_y}{Q}\right)^2\right](S_-^y + S_+^y) + \left[1-\left(\frac{Q_z}{Q}\right)^2\right](S_-^z + S_+^z). \tag{16d}$$

Taking into account the nearly perfect planar symmetry in the yz plane perpendicular to the direction of the applied field, one should have the following relations between the various ''partial'' structure factors and correlation lengths: $S_-^y \approx S_+^y \approx S_-^z \approx S_+^z \approx S_{yz}/2$ and $\xi_y \approx \xi_z \approx \xi_{yz}$. At $\mathbf{q}=\mathbf{k}_{\rm AF}$, S_ν and ξ_ν (with $\nu=x,yz$) should fulfill $S_0^x \propto \xi_x$ and $S_{yz} \propto \xi_{yz}$. It is easy to show that these relations imply the simple relations:

$$\Sigma I \propto (\xi_x + \xi_{yz}), \tag{17a}$$

$$I_- \approx I_+ \approx S_{yz}/2 \propto \xi_{yz}/2, \tag{17b}$$

$$I_0 \propto \xi_x . \tag{17c}$$

The fact that ΣI is experimentally independent of the field means that one should have from (17a) $\xi_x + \xi_{yz} \approx$const, a result also found in the spin-1 NENP (Ref. 76) and spin-5/2 TMMC (Ref. 79) chain compounds. In addition, the fact that experimentally one has $I_- \approx I_+ \approx I_0/2$ implies necessarily from (17b) and (17c) that $S_{yz} \approx S_x$ and $\xi_x \approx \xi_{yz}$. Consequently, our experimental results under field can be understood by assuming *weak* field dependences of the various correlation lengths and structure factors, which moreover remains nearly *isotropic* at the magnetic-field values explored. Further INS experiments will be necessary to confirm this viewpoint, in particular by improving the resolution in energy and carrying out measurements at higher fields (120 kOe is now available). Finally, we emphasize that the INS data of Fujita *et al.*[75] obtained below 60 kOe can be analyzed in a very similar manner, confirming the very weak anisotropy of $CuGeO_3$.

V. CONCLUSION

We have described exhaustive inelastic-neutron-scattering experiments on the inorganic spin-Peierls system $CuGeO_3$ performed in zero field and under an applied magnetic field. Our experimental investigation mainly concerned the lattice distortion associated with the SP transition and the magnetic excitation spectrum. Concerning the former, our results confirm unambiguously the existence of a structural distortion below a transition temperature $T_{\rm SP} \approx 14.2$ K, characterized by a propagation vector $\mathbf{k}_{\rm SP}=(1/2,0,1/2)$. Except for a shift in $T_{\rm SP}$, which was found to decrease quadratically with field, very weak changes were observed in the other lattice quantities at the magnetic fields which were applied (i.e., up to 100 kOe). In the standard model, the lattice distortion (triggered by the antiferromagnetic correlations) should be associated with a phonon softening. Such a feature could not be observed in organic prototypical SP systems such as TTF-CuBDT, essentially because of a lack of large single crystals absolutely needed in the INS experiments. The only signature of lattice effects was the existence in the x-ray patterns of diffuse scattering originating from pretransitional structural fluctuations, persisting up to relatively high temperatures comparatively to $T_{\rm SP}$. Very similar features were observed by x-ray diffraction in $CuGeO_3$, although with relatively small intensities. In contrast to these observations, *no* structural pretransitional fluctuations could be detected by neutron diffraction, even for temperatures very close to $T_{\rm SP}$. Moreover, despite careful measurements, no one, to our knowledge, has succeeded in observing any phonon softening in this material. Although the extreme weakness of the expected intensities could explain these results, we believe that the nature of the transition itself may play a role. In the standard theory, the nature of the transition is essentially of displacive type. In $CuGeO_3$, the possibility remains that the transition may be of order-disorder type. In this case, a broad quasielastic contribution should exist above the transition temperature, which would be very important to detect. In our opinion, polarized INS experiments would allow this observation. Below $T_{\rm SP}$, new phonon modes should appear in the vicinity of $\mathbf{k}_{\rm SP}$, which would be equally crucial for a better understanding of the SP mechanism in $CuGeO_3$.

Our investigation under field of the lattice distortion has revealed very weak changes, which in fact are not inconsistent with the standard theory. The interesting phenomena are expected to occur above H_c. Unfortunately, in $CuGeO_3$ the observed value of $H_c \approx 125$ kOe will strongly limit further investigation by neutron diffraction, the maximum field reachable in such measurements being by now about 120 kOe. Above H_c, incommensurability should take place both for the lattice distortion and the staggered magnetic component. In $CuGeO_3$, one expects a magnetic long-range ordering induced by the finite interchain couplings existing in this material. As previously mentioned, these features will be very difficult to observe directly by neutron scattering.

Concerning the magnetic counterpart, the situation turned out to be much clearer and unambiguous. Our measurements have confirmed the existence of a gap at the antiferromagnetic point $\mathbf{k}_{\rm AF}=(0,1,1/2)$ in the magnetic excitation spectrum, at a value $\Delta \approx 2$ meV ≈ 3.3–$3.4 k T_{\rm SP}$. In agreement with the standard theory, the gap value is quantitatively related to the transition temperature through a BCS-type relation. In $CuGeO_3$, the nonmagnetic ground state and the magnetic excitation spectrum can be reasonably well understood from a model based on a quasi-ideal alternating chain, despite the existence of sizable interchain couplings. Such a model explains more than qualitatively both the dispersion relation and the equal-time structure factor $S(q)$, and has allowed a very realistic determination of the exchange parameters ($2J_1 \approx 10.5$ meV and $\alpha \approx 0.9$–0.92). Quite interestingly, the continuum predicted theoretically, at least for sufficiently small values of $1-\alpha$, seems to have been observed in our experiments. However, additional work is necessary to confirm this feature, in particular by improving the resolution in energy and using polarized neutron scattering.

A central question, related to the search for an explanation for the unusual shape of $\chi(T)$, has addressed the possible existence of a pseudogap in the excitation spectrum above $T_{\rm SP}$. Our measurements seem to indicate the presence of such a feature at $\mathbf{q}=\mathbf{k}_{\rm AF}$, but in a relatively small temperature range above $T_{\rm SP}$. At higher temperatures, the pseudogap

is rapidly masked by the damping but nevertheless seems to vanish. Our experimental results suggest that the pseudogap starts to develop only when the structural intrachain correlation length becomes larger than typically $10c$. At $\mathbf{q}=\mathbf{k}_{SP}$, a clear inelasticity persists above the SP transition, which was ascribed to the low-dimensional character of the magnetism in $CuGeO_3$.

Under field, following a quite general scenario, the excited triplet is split into three components displaying linear dependences at the values of H which were measured. *Stricto sensu*, the observed behavior is very characteristic of that of an alternating chain, as if the spin-lattice couplings effects were very weakly relevant at low temperature. Our measurements below $0.77H_c$ have not brought much information concerning the magnetoelastic couplings present in $CuGeO_3$ for the essential reason that the magnetic and lattice components appear more or less decoupled in this field range. As discussed previously, stronger effects are expected in the vicinity of H_c. Of course, the most interesting thing would be to measure the magnetic excitation spectrum from INS in the incommensurate phase. Unfortunately, such experiments are unfeasible to date, for instrumental reasons. Finally, the most important effects were observed as a function of temperature. There are at least two points not really understood in this compound. The first one concerns the shape of $\chi(T)$ above T_{SP}, which is far from following the Bonner-Fisher law expected for a uniform chain. The second one is related to the ''anomalous'' disappearance of the lattice order parameter (i.e., $\langle\delta\rangle_T$). Experimentally, in the vicinity of T_{SP}, $\langle\delta\rangle_T$ has been shown to obey a power-law relation of type $\langle\delta\rangle_T \propto (T_{SP}-T)^{\beta}$, with an exponent $\beta \approx 0.26$, far from the mean-field value. We believe that these two features are signatures of the relevance of structural correlations, which persist up to relatively high temperatures (at least up to $3T_{SP}$).

From a theoretical point of view, the problem is now to go beyond the mean-field approximation and to try to incorporate these structural fluctuations. In fact, a clear understanding of the physical properties of $CuGeO_3$ would require the inclusion of the interchain couplings along the b direction, found to be relatively important ($|J_b'/J| \approx 0.1$). An additional complication could result from the necessity of taking into account the second neighbor *intrachain* couplings. It is possible that such interactions are relatively sizable in $CuGeO_3$, since the corresponding Cu-Cu distance (of the order of 5.9 Å) is not very large, and also because the associated AF superexchange paths involve Cu-O-O-Cu bonds which could allow sufficiently strong overlaps of atomic orbitals. In fact, in the germanate $CuGeO_3$, the intrachain interactions between first neighbors turned out to be relatively *small*. The present experimental determination gave $2J \approx 120$ K, a value which is more than one order of magnitude smaller than in the well-known 2D magnetic cuprates such as La_2CuO_4 or $YBa_2Cu_3O_6$ (see Refs. 80 and 81) although the Cu-Cu distance is much shorter (2.94 Å in $CuGeO_3$ instead of 3.8 Å in the cuprates). The combination of both effects could make the ratio of second-neighbor to first-neighbor intrachain exchange interactions relatively important (i.e., of order of 1/4). Since this ratio is believed to induce quantum disorder, if it is sufficiently strong, one may anticipate it to go against the interchain couplings and restore the singlet ground state. This has to be quantitatively demonstrated, however.

ACKNOWLEDGMENTS

We would like to thank J. P. Boucher, T. Brill, D. Grempel, K. Hirota, Th. Jolicoeur, E. Lorenzo, P. Pfeuty, J. P. Pouget, J. P. Renard, and I. Zaliznyak for numerous and illuminating discussions. It is a pleasure to thank B. Fåk for his help with the manuscript. A.R. and G.D. acknowledge NEDO for financial support. Laboratoire de Chimie des Solides is ''Unité de Recherche Associée au CNRS n°446.''

[1] H. Bethe, Z. Phys. **71**, 205 (1931).
[2] J. Des Cloiseaux and J. J. Pearson, Phys. Rev. **128**, 2131 (1962).
[3] T. Yamada, Prog. Theor. Phys. Jpn. **41**, 880 (1969).
[4] G. Müller, H. Beck, and J. C. Bonner, Phys. Rev. Lett. **43**, 75 (1979).
[5] E. Pytte, Phys. Rev. B **10**, 2309 (1974).
[6] J. W. Bray, H. R. Hart, L. V. Interrante, I. S. Jacobs, J. S. Kasper, G. D. Watkins, S. H. Wee, and J. C. Bonner, Phys. Rev. Lett. **35**, 744 (1975).
[7] M. C. Cross and D. S. Fisher, Phys. Rev. B **19**, 402 (1979).
[8] R. A. T. de Lima and C. Tsallis, Phys. Rev. B **27**, 6896 (1983).
[9] J. C. Bonner and H. W. J. Blöte, Phys. Rev. B **25**, 6959 (1982).
[10] L. N. Bulaevskii, Sov. Phys. JETP **16**, 685 (1963).
[11] W. Duffy and K. Barr, Phys. Rev. **165**, 647 (1968).
[12] C. Tannous, Phys. Rev. B **32**, 4770 (1985).
[13] D. Grempel *et al.* (unpublished).
[14] L. N. Bulaevskii, A. I. Buzdin, and D. I. Khomskii, Solid State Commun. **27**, 5 (1978).
[15] M. C. Cross, Phys. Rev. B **20**, 4606 (1979).
[16] J. W. Bray, Solid State Commun. **26**, 771 (1978).
[17] I. Harada and A. Kotani, J. Phys. Soc. Jpn. **51**, 1737 (1982).
[18] I. Affleck, Phys. Rev. B **41**, 6697 (1990).
[19] O. Golinelli, Th. Jolicoeur, and R. Lacaze, J. Phys. Condens. Matter **5**, 7847 (1993).
[20] T. Sakai, J. Phys. Soc. Jpn. **64**, 251 (1995).
[21] I. S. Jacobs, J. W. Bray, H. R. Hart, L. V. Interrante, J. S. Kasper, G. D. Watkins, D. E. Prober, and J. C. Bonner, Phys. Rev. B **14**, 3036 (1976).
[22] J. A. Northby, H. A. Groenendijk, L. J. de Jongh, J. C. Bonner, I. S. Jacobs, and L. V. Interrante, Phys. Rev. B **25**, 3215 (1982).
[23] S. Huizinga, J. Kommandeur, G. A. Savatzky, B. T. Thole, W. J. M. de Jonge, and J. Roos, Phys. Rev. B **19**, 4723 (1979).
[24] I. S. Jacobs, H. R. Hart, L. V. Interrante, J. W. Bray, J. S. Kasper, G. D. Watkins, D. E. Prober, W. P. Wolf, and J. C. Bonner, Physica B **86–88**, 655 (1977).
[25] D. Bloch, J. Voiron, J. C. Bonner, J. W. Bray, I. S. Jacobs, and L. V. Interrante, Phys. Rev. Lett. **44**, 294 (1980).
[26] D. Bloch, J. Voiron, J. W. Bray, I. S. Jacobs, J. C. Bonner, and J. Kommandeur, Phys. Lett. **82A**, 21 (1981).
[27] L. S. Smith, E. Ehrenfreund, A. J. Heeger, L. V. Interrante, J. W. Bray, H. R. Hart, and I. S. Jacobs, Solid State Commun. **19**, 377 (1976).

[28] J. S. Kasper and D. E. Moncton, Phys. Rev. B **20**, 2341 (1979).
[29] W. A. C. Erkelens, L. P. Regnault, J. Laugier, J. Rossat-Mignod, and L. J. de Jongh, Solid State Commun. **55**, 209 (1985).
[30] Q. Liu, S. Ravy, J. P. Pouget, C. Coulon, and C. Bourbonnais, Synth. Met. **55–57**, 1840 (1993).
[31] J. W. Bray, L. V. Interrante, I. S. Jacobs, D. Bloch, D. E. Moncton, G. Shirane, and J. C. Bonner, Phys. Rev. B **20**, 2067 (1979).
[32] V. Kiryukhin, B. Keimer, and D. E. Moncton, Phys. Rev. Lett. **74**, 1669 (1995).
[33] M. Hase, I. Terasaki, and K. Uchinokura, Phys. Rev. Lett. **70**, 3651 (1993).
[34] M. Hase, I. Terasaki, K. Uchinokura, M. Tokunaga, N. Miura, and H. Obara, Phys. Rev. B **48**, 9616 (1993).
[35] M. Nishi, O. Fujita, and J. Akimitsu, Phys. Rev. B **50**, 6508 (1994).
[36] L. P. Regnault, M. Aïn, B. Hennion, G. Dhalenne, and A. Revcolevschi, Physica B **213 & 214**, 278 (1995).
[37] K. Hirota, D. E. Cox, J. E. Lorenzo, G. Shirane, J. M. Tranquada, M. Hase, K. Uchinokura, H. Kojima, Y. Shibuya, and T. Tanaka, Phys. Rev. Lett. **73**, 736 (1994).
[38] J. E. Lorenzo, K. Hirota, G. Shirane, J. M. Tranquada, M. Hase, K. Uchinokura, H. Kojima, I. Tanaka, and Y. Shibuya, Phys. Rev. B **50**, 1278 (1994).
[39] J. Kikuchi, Y. Yasuoka, M. Hase, Y. Sasago, and K. Uchinokura, J. Phys. Soc. Jpn. **63**, 872 (1994).
[40] K. Le Dang, G. Dhalenne, J. P. Renard, A. Revcolevschi, and P. Veillet, Solid State Commun. **91**, 927 (1994).
[41] T. M. Brill, J. P. Boucher, J. Voiron, G. Dhalenne, A. Revcolevschi, and J. P. Renard, Phys. Rev. Lett. **73**, 1545 (1994).
[42] S. Sahling, J. C. Lasjaunias, P. Monceau, and A. Revcolevschi, Solid State Commun. **92**, 423 (1994).
[43] S. B. Oseroff, S. W. Cheong, B. Atkas, M. F. Hundley, Z. Fisk, and L. W. Rupp, Jr., Phys. Rev. Lett. **74**, 1450 (1995).
[44] K. Kuroe, T. Sekine, M. Hase, Y. Sasago, K. Uchinokura, H. Kojima, I. Tanaka, and Y. Shibuya, Phys. Rev. B **50**, 16 468 (1994).
[45] J. P. Pouget, L. P. Regnault, M. Aïn, B. Hennion, J. P. Renard, P. Veillet, G. Dhalenne, and A. Revcolevschi, Phys. Rev. Lett. **72**, 4037 (1994).
[46] O. Kamimura, M. Terauchi, M. Tanaka, O. Fujita, and J. Akimitsu, J. Phys. Soc. Jpn. **63**, 2467 (1994).
[47] J. C. Bonner and M. E. Fisher, Phys. Rev. **135**, A 640 (1964).
[48] H. Vollenkle, A. Wittmann, and H. Nowotny, Monatsh. Chem. **98**, 1352 (1967).
[49] A. Revcolevschi and R. Collongues, C R. Acad. Sci. **266**, 1767 (1969).
[50] A. Revcolevschi, Rev. Int. Hautes Temp. Refract. **7**, 73 (1970).
[51] M. Horvatic *et al.* (unpublished).
[52] E. Ehrenfreund and L. S. Smith, Phys. Rev. B **16**, 1870 (1977).
[53] Q. J. Harris, Q. Feng, R. J. Birgeneau, K. Hirota, K. Kakurai, J. E. Lorenzo, G. Shirane, M. Hase, and K. Uchinokura, Phys. Rev. B **50**, 12 606 (1994).
[54] M. Nishi, O. Fujita, and J. Akimitsu, J. Phys. Soc. Jpn. (to be published); Physica B (to be published).
[55] K. Hirota, R. J. Birgeneau, M. Hase, H. Kojima, J. E. Lorenzo, Y. Shibuya, G. Shirane, I. Tanaka, J. M. Tranquada, and K. Uchinokura, Physica B **213 & 214**, 284 (1995).
[56] M. Aïn, B. Hennion, L. P. Regnault, G. Dhalenne, and A. Revcolevschi (unpublished).
[57] C. K. Majumdar and D. K. Ghosh, J. Math. Phys. **10**, 1399 (1969).
[58] F. D. M. Haldane, Phys. Rev. B **25**, 4925 (1982); **26**, 5257 (1982).
[59] T. Tonegawa and I. Harada, J. Phys. Soc. Jpn. **56**, 2153 (1987).
[60] R. R. P. Singh, P. A. Fleury, K. B. Lyons, and P. E. Sulewski, Phys. Rev. Lett. **62**, 2736 (1989).
[61] S. Ma, C. Broholm, D. H. Reich, B. J. Sternlieb, and R. W. Erwin, Phys. Rev. Lett. **69**, 3571 (1992).
[62] K. Okamoto, J. Phys. Soc. Jpn. **56**, 913 (1987); **56**, 1627 (1987).
[63] K. Nomura, Phys. Rev. B **40**, 2421 (1989).
[64] P. C. Hohenberg and W. F. Brinkman, Phys. Rev. B **10**, 128 (1974).
[65] I. Affleck, T. Kennedy, E. H. Lieb, and H. Tasaki, Phys. Rev. Lett. **59**, 799 (1987).
[66] D. P. Arovas, A. Auerbach, and F. D. M. Haldane, Phys. Rev. Lett. **60**, 531 (1988).
[67] D. Dorner, Acta. Crystallogr. A **28**, 319 (1972).
[68] J. E. Lorenzo (private communication).
[69] J. P. Renard, K. Le Dang, P. Veillet, G. Dhalenne, A. Revcolevschi, and L. P. Regnault, Europhys. Lett. **30**, 475 (1995).
[70] M. Steiner, J. Villain, and G. Windsor, Adv. Phys. **25**, 87 (1976).
[71] K. Hirakawa, H. Yoshizawa, J. D. Axe, and G. Shirane, J. Phys. Soc. Jpn. **52**, 4220 (1983).
[72] L. P. Regnault and J. Rossat-Mignod, in *Magnetic Properties of Layered Metal Compounds*, edited by L. J. de Jongh (Kluwer, Amsterdam, 1990), pp. 271–321.
[73] L. P. Regnault, I. Zaliznyak, and S. Meshkov, J. Phys. Condens. Matter **5**, L677 (1993).
[74] H. J. Schultz (private communication).
[75] O. Fujita, J. Akimitsu, M. Nishi, and K. Kakurai, Phys. Rev. Lett. **74**, 1667 (1995).
[76] L. P. Regnault, I. Zaliznyak, J. P. Renard, and C. Vettier, Phys. Rev. B **50**, 9174 (1994).
[77] S. W. Lovesey, in *Theory of Neutron Scattering from Condensed Matter* (Clarendon, Oxford, 1984), Vols. 1 and 2.
[78] I. Affleck, Phys. Rev. B **46**, 9002 (1992).
[79] J. P. Boucher, L. P. Regnault, J. Rossat-Mignod, J. Villain, and J. P. Renard, Solid State Commun. **31**, 311 (1979).
[80] S. Shamoto, M. Sato, J. M. Tranquada, B. J. Sternlieb, and G. Shirane, Phys. Rev. B **48**, 13 817 (1993).
[81] G. Aeppli, S. M. Hayden, H. A. Mook, T. E. Mason, A. D. Taylor, K. N. Klausen, T. G. Perring, S. W. Cheong, Z. Fisk, and D. Rytz, Physica B **192**, 103 (1993).